MACHINE LEARNING & DATA ANALYTICS

FRIEDRICH-ALEXANDER UNIVERSITÄT ERLANGEN-NÜRNBERG
TECHNISCHE FAKULTÄT

Macro Analysis of free-living Gait in Parkinson's Disease

Bachelor's Thesis in Medical Engineering

submitted
by

Stefan Michael Fischer

born 02.06.1996 in Kronach

Written at

Machine Learning and Data Analytics Lab (CS 14)
Department of Computer Science
Friedrich-Alexander-Universität Erlangen-Nürnberg (FAU)

Advisors:
Martin Ullrich M. Sc., Dr.-Ing. Felix Kluge, Prof. Dr. Björn Eskofier
(Machine Learning and Data Analytics Lab, FAU Erlangen-Nürnberg)
Dr. phil. Heiko Gaßner
(Department of Molecular Neurology, Univeristy Hospital Erlangen)

Started: 01.12.2018

Finished: 30.04.2019

Ich versichere, dass ich die Arbeit ohne fremde Hilfe und ohne Benutzung anderer als der angegebenen Quellen angefertigt habe und dass die Arbeit in gleicher oder ähnlicher Form noch keiner anderen Prüfungsbehörde vorgelegen hat und von dieser als Teil einer Prüfungsleistung angenommen wurde. Alle Ausführungen, die wörtlich oder sinngemäß übernommen wurden, sind als solche gekennzeichnet.

Die Richtlinien des Lehrstuhls für Bachelor- und Masterarbeiten habe ich gelesen und anerkannt, insbesondere die Regelung des Nutzungsrechts.

Erlangen, den 30.04.2019

Übersicht

Durch die stetige Weiterentwicklung von Beschleunigungssensoren und der damit einhergenden Kostensenkung und längeren Operationszeit werden diese immer häufiger im Umfeld von Home-Monitoring Ganganalyse-Systemen genutzt. Ziel ist dabei, durch den Anstieg von Daten vermehrt klinisch relevante Informationen zu generieren, um den Arzt bei Therapie und Diagnose der Parkinson Krankheit zu unterstützen. Standardisierte Gangtests werden nun nicht nur im klinischen Ganglabor, sondern mit dem Home-Monitoring System auch im Heim des Patienten durchgeführt. Ziel der Arbeit sind die Entwicklung von Algorithmen um 1) standardisierte Gangtests, den 4x10m Test und den zwei Minuten-Lauf, automatisch in den Home-Monitoring Daten zu erkennen und 2) Macroparameter aus dem freiem Gang der Home-Monitoring Daten zu berechnen, wobei Ergebnisse, produziert durch zwei verschiedene Definitionen von Gangsequenzen, miteinander verglichen werden. Für die automatische Gangtesterkennung wurde ein Datensatz aus 286 klinischen Ganguntersuchungen genutzt, um den Detektionsalgorithmus zu trainieren und zu evaluieren. Das Verfahren basiert auf einem Dynamic Time Warping Ansatz, welcher ein Eingabesignal mit einem vorgefertigten Muster vergleicht und ein quantitatives Ähnlichkeitsmaß ausgibt. Der Algorithmus liefert einen F1-score von 93.4 % beim Evaluieren auf dem Klinikdatensatz. Des Weiteren wurde die Erstellung des Musters analysiert und hinsichtlich der Dynamic Time Warping Distanzen optimiert, um das Übertragen der Methodik auf andere Sensorsysteme zu vereinfachen.

Auf der anderen Seite wurden Macroparameter wie Schritte pro Tag, Gangsequenzen pro Tag und die durchschnittliche Länge einer Gangsequenz pro Tag für einen Home-Monitoring Datensatz eines Parkinson-Patienten berechnet, welcher über 11 Tage lang aufgenommen wurde. Gangsequenzen wurden hierbei durch zwei Definition mit maximaler Ruhezeit von 10 oder 2.5 Sekunden generiert. Hierbei unterschieden sich die Macroparameter Gangsequenzen pro Tag um bis 63 ± 3 % und durchschnittliche Länge einer Gangsequenz pro Tag um 54 ± 8 %. Die Ergebnisse unterstützen Resultate anderer Studien und verdeutlichen die Benötigung einer festen Definition von Gangsequenzen innerhalb der Forschung.

Der in der Thesis vorgestellte Algorithmus ist, soweit uns bekannt ist, der Erste in dem Anwendungsfeld der automatischen Erkennung von standardisierten Gangtest und schafft die Möglichkeit der einfachen Nutzung eines Home-Monitoring Systems, ohne das Zeitmarker manuell gesetzt werden müssen, welche Gangtests kennzeichnen.

Abstract

Due to the continous progress in manufacturing of inertial sensors and therefore sinking of costs and extention of operation time, those sensors get used more often in the field of home-monitoring systems for gait analysis. The goal of home-monitoring is improving the clinical outcomes by acquiring more data to support the clinician with the diagnosis and therapy of Parkinson's Disease. Standardized gait tests are not only recorded in the clinical environment, but also in the patient's home, as the subject can be recorded with the home-monitoring system. Goals of this thesis were the development of algorithms that 1) are able to detect standardized gait tests, which are the 4x10m test and the two minute walking test, from continous sensor data and 2) to calculate macro parameters from free-living gait, where results of two different walking bout definitions are compared. For the automatic test detection there was a data set of 286 clinical gait sessions to train and evaluate the algorithm. The method is based on a dynamic time warping approach, which compares an input signal with a predefined template and quantifies similarity between both. Therefore, the creation of templates was analyzed and optimized on the dynamic time warping distances to ease the applying of this method to other sensor systems. The classification scored a F1-measure of 93.4 % for evaluation on the clinical sessions.

On the other hand, macro parameters like steps per day, walking bouts per day and the mean walking bout length were calculated on the home-monitoring data of one Parkinson's disease patient, recorded over 11 days. Walking bouts were created with two walking bout definitions of maximum resting time of 10 or 2.5 seconds. The macro parameter number of bouts per day differs by 63 ± 3 %, while mean bout length differs by 54 ± 8 %. The results support findings other studies and point up to the importance of a general walking bout definition within research.

The developed algorithm is to the best of our knowledge the first algorithm in the field of automatic gait test detection and creates the possibilty of easy use of the home-monitoring system, without manual setting of time stamp annotations, which identify gait tests.

Contents

Chapter 1

Introduction

1.1 Motivation

Parkinson's Disease (PD) is a neurodegenerative disorder of the central nervous system which also affects the motor system. Impaired subjects suffer from gait disorders and balance impairments [Boo08], associated with falls and reduced quality of life [Blo04]. Especially falls can lead to injuries like hip fractures and average life expectancy is reduced to approximately 7 years, once recurrent falls are present [Blo01].

To assess movement disorders, PD impaired patients get evaluated by clinical experts with different rating scales like the Unified Parkinson Disease Rating Scale part III (UPDRS-III) [Goe08] and the Hoehn & Yahr (H&Y)[Goe04]. Drawbacks of those clinical rating scales are the time dependence and the subjectivity due to rating by doctors [Klu13]. One alternative evaluation to ratings by experts is the screening of neurological diseases by different motion recording systems. Thus, quantitative measures related to motion are available.

Clinical experts use standardized gait tests to assess the patients' gait. Additionally there are also specific gait tests which where created for quantitative evaluation of sensor data. Outcome parameters like velocity, stride length and stride time are good prognostic indicators for fall risk and bad health outcomes [Bro17, Lor16, Sch14, Ash01, Wil06].

The gold standard sensor systems are optical systems, but they requiere laboratory settings and are also expensive. To overcome these limitations intertial measurement units (IMUs) are used by a lot of researchers [Che16, Heg16, Rov17, Esk17]. Low prices and long operating times of inertial sensors additionally realize the possibility of home-monitoring [Bjo07, Cav07, McD05, Sab05, Tao12].

Due to an increase of available motion data by long-term monitoring, fall risk prediction

could improve with home-monitoring [Bro17, Zam11, Del17]. The recorded data is processed differently than the processing of instrumented gait tests. On the one side when evaluating clinical gait tests, results in calculation of parameters linked to single strides. Those parameters are called micro parameters in current research [Del17]. On the other side relations between intervals of linked strides over one day can be calculated. The term macro parameters refers to those parameters [Del17]. In literature different definitions of intervals of linked strides exists, causing problems comparing research results easily [Bar15, Del16]. Those specific intervals are called walking bouts (WB).

Current work on home-monitoring is done at the Machine Learning and Data Analytics Lab of Friedrich-Alexander-University Erlangen-Nuremberg. In the project "FallRiskPD" a home-monitoring concept is being developed to predict falls in PD patients. In this project subjects wear inertial sensors and also perform gait tests in their home-environment over the time of two weeks. Furthermore, patients manually set time stamp annotations while performing gait tests. Therefore, tests can be segmented from the long-term data and the patients' gait micro characteristics during those tests can be computed. As PD is age-related, most of the studies participants are elderly persons, leading to greater amount of incorrect labels [Zar02], which effects outcomes of the micro analysis.

1.2 Related Work

In this section previous research which is related to topics of this thesis are presented.

1.2.1 Gait Tests in Home-Environments

Considering the fact that clinical gait differs from free-living gait [Bro16], there were studies which observed if gait tests at home are feasible and reliable. Lim et al. performed timed up and go tests (TUG) and a timed walking tests in patients' environments [Lim05]. Three observers and 26 PD patients (age = 62.5 $\pm$ 8.2 years) were part of the study cohort. By calculation of intraclass correlation and intra/inter observer reliability, their results support the claim that gait tests in home-environments are feasible. Furthermore Lim et al. suggest standardized practical guidelines for less optimal circumstances like the home-environment.

Another study concerning those specific gait tests was carried out by Zampieri et al. [Zam11]. One goal was to test feasability of instrumented gait tests at home. Furthermore they investigated micro parameter differences in home-environments and clinical-environments using inertial sensors (Physilog^{TM}; GaitUp SA; Lausanne; Switzerland). A small study cohort of six PD

patients (age = 57.3 $\pm$ 8.6 years) and eight healthy controls (age = 63.7 $\pm$ 5.9 years) performed instrumented TUG tests. Calculated micro parameters were stride velocity, stride length, cadence and turning velocity. Statistical analysis was executed with repeated measures ANOVA for groups PD vs Control subjects. Like the outcomes of Lim et al. outcomes of Zampieri et al. also support the feasibilty of gait tests at home, in the case of Zampieri et al. also instrumented gait tests. In the work of Zampieri et al. test-retest reliability was ranging between good and excellent for five different micro parameters ($\rho = 0.83 \pm 0.1$). Furthermore they detected that PD subjects' performance are more affected than parameters of the controls. Zampieri et al. also stated possible reasons. For instance, home-environments are more cluttered and constrained than laboratory settings. Moreover, most of the subjects feel more comfortable and relaxed at home.

1.2.2 Walking Bouts Definitions in Literature

In literature there are different definitions of one walking bout. The names of those intervals are also varying, as ambulatory bouts and walking periods are referring to the same meaning [Del16, Del17, Naj03]. A WB is an interval of successive strides [Del17, Ore08, Dan14, Roo12, Sch14, Naj03, Del16, TL12]. In most research works those intervals have a minimum number of strides and end after a specific period of time in which no stride occured. Minimum stride amounts are sometimes set to two successive strides [Ore08, Dan14] but mostly three successive strides [Del16, Del17, Roo12, Sch14, Naj03, TL12]. Different definitions appear regarding the amount of time a resting period lasts till the WB ends. The values range from 2.5 seconds up to more than 60 seconds [Del16, Wei13, Bro15, Bro16, Sch14]. This leads to problems in comparing results easily. Another factor influencing the WB definion comes with the sensor setup. Orendurff et al. were using a maximum resting period (MRP) of 10 seconds, limited by the used technology (Stepwatch Activity Monitor; OrthoCare Innovations; Mountlake Terrace, Washington) [Ore08].

The work of Barry et al. concering different resting time values and how they affect the outcomes supports that those definitions are crucial [Bar15]. Their study cohort contained 97 older adults (age = 69.2 $\pm$ 7.7 years) and gait was assessed using an accelerometer (activPAL^{TM}; PAL Technologies Ltd; Strathclyde; Scotland) worn on the upper thigh over 7 successive days. For instance, modifying the MRP has large impacts on volume, patterns and variabilty measures. By setting the MRP to 6 seconds only 6 % of their study cohort fullfilled public health guidelines. Despite that by raising the MRP to 30 seconds already 40 % of the subjects fullfilled guidelines. Therefore, methods to compare studies performed with different walking bout definitions are from great interest like the regression method of Barry et al. [Bar15].

1.2.3 Macro Parameters in Literature

Measuring human locomotion can have useful output, as gait varies with overall health [Lor13a], cognitive decline [Ver07], falls status [Bea09] and longevity [Stu11]. Furthermore gait measurement is noninvasive, relatively low cost and the objective quantitative results can support the clinician in diagnosis and disease managements [Lor13a]. In addition to micro gait characteristics, which are recorded in the clinic, free-living behavioural gait characteristics can be quantified using the same sensors. Analysis of those free-living gait characteristics is also called macro analysis [Del17]. By examining broader trends of gait signals, different macro parameters can be quantified. Moreover finding relations between those macro characteristics and clinical outcomes, like disease diagnosis, disease progression and fall risk, are of great interest.

In the field of macro gait analysis there are different parameters which are of high interest. By assessing WBs, macro parameters like volume, pattern and variability of those WBs can be calculated [Del16, Del17]. Del Din et al. showed that there are significant differences in macro paramters comparing PD patients and age-matched controls. Their study cohort of 47 (age = 69.1 $\pm$ 8.3 years) PD patients and 50 controls (age = 69.8 $\pm$ 7.2 years) was recorded with a single tri-axial accelerometer (Axivity AX3; York; UK) on the lower back for 7 days. They found that free-living conditions heightened between-group differences and that those differences are more prominent in walking bouts of longer durations (WBs $\geq$ 10 seconds). For comparing those macro parameters they also suggest laboratory tests of longer walking durations.

1.3 Purpose of the Thesis

The goal of this thesis is to develop tools to process long-term gait data collected in the home environment during the FallRiskPD study. Besides their usual activities of daily living, the participating PD patients are instructed to perform specific clinical gait tests in their home environment. Automatic detection of those gait tests in the continous data will improve usability of our home-monitoring system by saving up time and easier operation. Furthermore, automatic test detection will generate more accurate time stamps of start and end of gait tests in the data, which leads to more precise outcomes by instrumented gait tests.

Moreover by segmentating detected gait tests from home-monitoring data, the remaining data is free-living gait. Broader trends of movement in this free-living gait are represented quantitatively by macro parameters. By calculating those parameters additional clinical relevant informations are collected. A drawback is, that different definitions of WB, which are needed for macro parameter calculation, are used presently leading to comparison difficulties [Bar15].

Furthermore, macro parameters are highly depending on the used WB definition. Therefore, two different WB definitions were used in this thesis to compute WBs and compare their effect on outcome parameters.

Chapter 2

Background

In the following sections the relevant background regarding PD, human gait and sensor based gait analysis will be discussed. The information of this chapter will be used in the following chapters: On the one side a method for detecting gait tests is investigated. On the other side macro parameters of PD patients, screened with a home-monitoring system, are calculated.

2.1 Parkinson's Disease

Parkinson's disease is a neurodegenerative disease, which is initiated by an interaction of genetic and exogenous factors [Wei09]. Due to an ongoing dying of specific brain cells which produce proteins, there is lack of the neurotransmitter dopamin [Bra06]. Resulting from a loss of those brain cells, located in the Substantia Nigra, the diseased person will develop motion impairments beside other symtomps [Sni07]. With the progression of the disease those movement difficulties will increase and are used to determine the disease stage [Ram02]. As nowadays PD is still incureable, the only way to improve the patient's situation is to reduce impairments by medication [Wor13]. Depending on the disease stage the doctor can also adapt the medication to improve the outcome of the therapy . The current workflow for the patient is to come to a hospital to get his current status evaluated by a professional, also investigating his motion patterns using standardized rating scales. One of those scales is the Unified Parkinson's Disease Rating Scale (UPDRS), which was developed by Fahn et al [Bra06] and is state of the art [Goe08]. Another clinical scale is the Hoehn and Yahr (H&Y) scale which can be easily applied [Bhi12]. Those scales are the basis for medication and rate of the success of the ongoing therapy [Pos07]. Among all symptoms of PD, some symptoms have an direct impact on the gait pattern of those patients. Those cardinal symptoms are now described more in detail.

2.1.1 Cardinal Symptoms

The following four symptoms are very common in PD and are observed to stage the disease progression.

Bradykinesia

Bradykinesia, the slowness of performed movement, is the most characteristic symptom in PD. Including difficulties in planning, initation and execution of movement, this symptom leads to increasing reaction time . Especially self-paced movements pose a problem for PD patients [Ber01].

Resting Tremor

The resting tremor is a noticable symptom giving PD the name shaking palsy. Extremities, especially in the distal parts of arms and legs start to shake. This symptom is already recognizable in early stages of the disease [Shu96].

Rigidity

Another PD related symptom is rigidity, which is commonly defined as a stronger resistance for joint movements like reflexion, rotation and extension [Bro07].

Postural Instability

More prominent in the late stage of PD, postural instability effects the patients postural reflexes, decreasing the balance. As a result the impaired person tends to fall [Wil06].

2.1.2 Resulting Gait Impairments

As a result PD patients develop characteristic gait disorders, due to cardinal symptoms. Those impairments lead to reduced step length and step height, resulting in a lower overall walking speed [Klu15]. Often parkinsonian gait is described as shuffling gait, emphasizing the character of the small step size walking [Sni07]. Another important aspect is the inscreasing problem of initating gait [Ros97, Hal98]. Further cardinal symptoms can lead to freezing of gait (FOG), which occurs mostly in gait initation [Gil01]. FOG can result in falling, leading to the fact that almost 70 % of the PD patients fall in a time span of one year and recurrent falls occur in about 50 % of all cases [Blo04]. Figure 2.1 displays the amount of falls of PD patients compared to healthy subjects. Study controls are age matched to PD patients. Subjects impaired with PD have much higher risks of falling and recurrence of those events. Hip fractures are the most feared consequences of falls and 25 % of all patients will develop one hip fracture within 10 years after the diagnose [Blo04].

Therefore, the quality of life sinks as the fear of falling increases over time and some patients are largely isolated [Sch00, Sch06, Mus08]. According to Bloem et al. average life expectancy is reduced to approximately 7 years, once recurrent falls take place [Blo04].

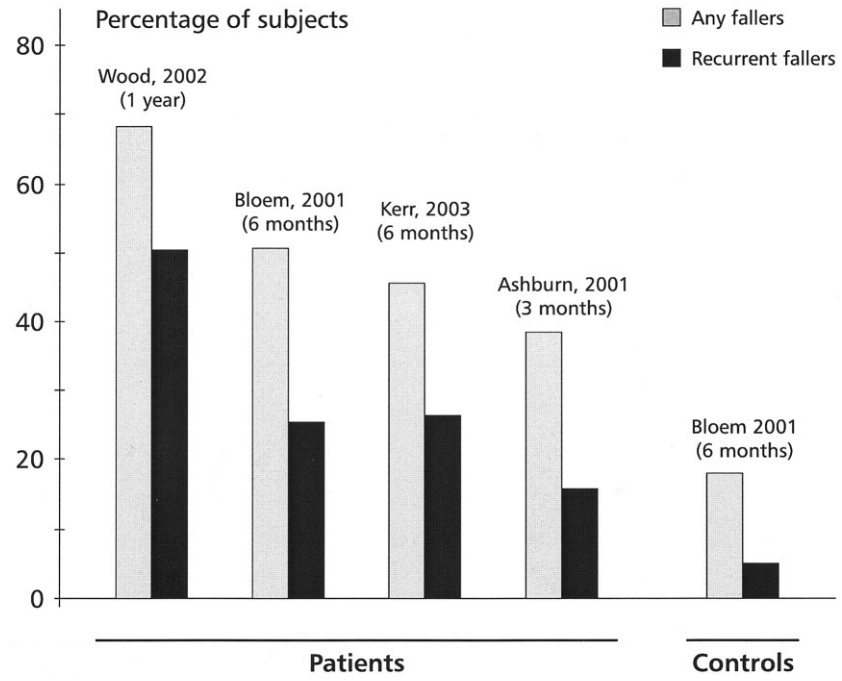

Figure 2.1: Fall Rates in PD. Four different studies [Woo02, Blo01, Ker10, Ash01] of falls related to PD.

2.2 Sensor Based Gait Analysis

The next section will cover an introduction to sensor-based recording of human gait. First of all, human gait is defined by its events and the according transitions. Afterwards, important instrumented gait tests and their output, quantified gait parameters, are discussed. Furthermore, the principles of inertial sensors are explained.

2.2.1 Human Gait

Human's upright gait is a complex movement pattern and it is characteristic for the human kind. To assess human gait as signal, there is a common methodology based on the following definitions by Beckers et al. [Bec97]. One stride is defined as the sequence between one heel-strike (HS) and the successive heel-strike (HS) of the same foot. A heel-strike is the moment, the heel hits the

ground. This gait sequence contains one heel-strike (HS), the mid-stance event (MS), the heel-off (HO) followed by the toe-off (TO). The last event before the sequence repeats with the next HS is the mid-swing. This gait cycle is illustrated by Figure 2.2. Next to that a step is defined as a HS of one foot till the HS of the other foot.

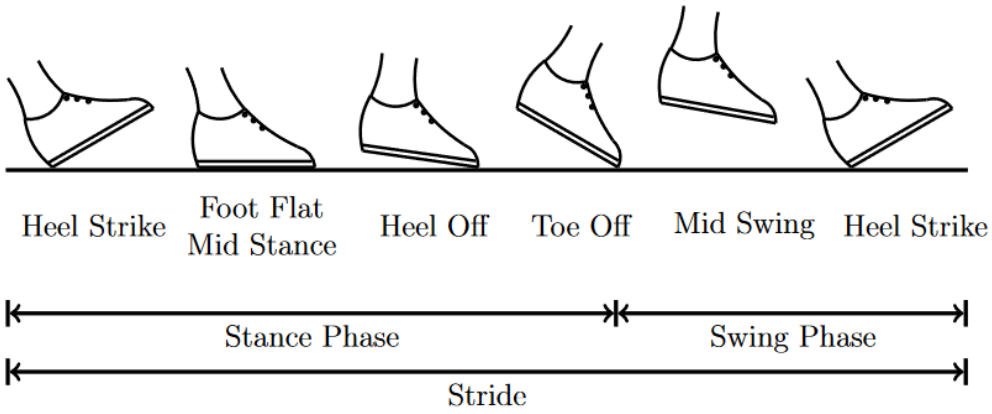

Figure 2.2: Human Gait Cycle. Illustration of the different gait events grouped to two gait phases. One periodic cycle is one stride [Kan14].

A gait cycle can also be divided into two phases of gait, also illustrated in Figure 2.2. During the stance phase the foot keeps contact with the ground. The stance phase starts with the HS and ends with the TO, describing the time during which the foot keeps contact with the ground. On the other hand is the swing phase, where the whole mass of the human is carried by the contalateral foot [Bar17]. One phase starts with the end of the other phase, in which the stance phase lasts around 60 % and the swing phase around 40 % of one gait cycle [Whi91].

2.2.2 Gait Parameters

For the evaluation of gait, different gait parameters are examined. A possible subdivision of gait parameters are micro and macro parameters [Del17]. This subdivision is based on WBs, which are intervals consisting of successive steps. Micro parameters can be calculated by micro-structural characteristics, which make up each WB and macro-structural characteristics consisting of all WBs of a long time-span such as one day. Examples for popular micro and macro parameters are shown in Table 2.1. As the term WB has no general definition in the literature, authors calculate different outputs for macro parameters, which leads to a generalization problem [Bar15]. This aspect will be further disscussed in the following chapters.

Table 2.1: Micro and Macro-Gaitparameters. Parameters from [Del17, Bar17] .

Parameter	Micro/Macro	Description
Stride Velocity	Micro	Velocity of subject during gait
Stride Length	Micro	Geometric length of one stride (HS to HS)
Stride/Swing/Stance Time	Micro	Time duration of gait phases
Total Walking Time per Day	Macro	Time volume of gait of one day
Number of Steps per Day	Macro	Amount of steps of one day
Number of Bouts per Day	Macro	Amount of bouts of one day
Mean Bout Time Duration	Macro	Mean time duration of all bouts
Bout Variability	Macro	Variability of pattern, length and density

2.2.3 Inertial Sensors

Inertial sensors are small eletrical devices, measuring acceleration and angular velocity of the device. Part of those sensors is a gyroscope which records angular velocity and an accelerometer which records the acceleration. Since recent improvements in micro-sensor manufacturing, inertial sensors have become applicable for a variety of fields. After miniaturization they are now used in a variety of applications like sports research, video game development and motion analysis for healthcare. The sensors collect data from the accelerometer and the gyroscope and each of them measures the three coordinate axes. In this thesis those sensors are used as a strapdown system. They are tightly attached onto the shoes and record the direct movement of the feet to collect free-living gait data.

The accelerometer records acceleration in anterior-posterior (a_{ap}), inferior-superior (a_{is}) and lateral-medial (a_{lm}) direction. Gyroscope record angular velocities of the rotations in coronal (g_{cor}), transverse (g_{trans}) and sagittal plane (g_{sag}).

Accelerometer

Micro-machined electromechanical accelerometers work on the same basis as mechanical accelerometers, which consist of a mass suspended by springs. Figure 2.3 shows a spring-mass system with pickoff. If the device gets accelerated, the mass is displaced against the springs. In electrical systems the displacement can be measured using capacitivity or piezoelectricity [Bao05]. By screening the displacement of the mass by the specific pickoff, the force on the mass can be calculated with the Hook's law:

$$F_d = D \cdot \Delta l \tag{2.1}$$

With the known spring constant D and the measured displacement Δl the force on the mass can be calculated by Newton's second law:

$$F = m \cdot a \tag{2.2}$$

Thus, the applied acceleration a along the corresponding axis can be calculated by measuring the mass' displacement [Woo02]. During constant velocity or rest, only gravity force has impact on the mass, giving information about inclination of the sensor regarding the horizontal plane. As output acceleration is relative to gravity, also the output value is often given relative to gravity.

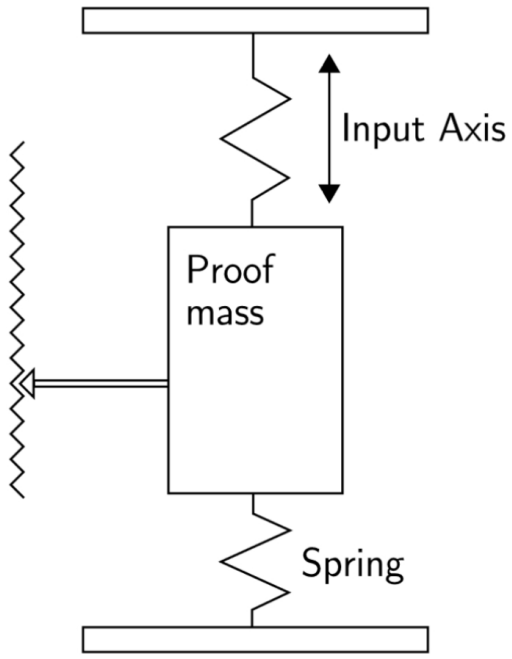

Figure 2.3: Mechanical Accelerometer. A mechanical accelerometer (spring-mass system). Acceleration can be measured corresponding the input axis [Woo02].

Gyroscope

Micro-machined electromechanical gyroscopes are based on the Coriolis effect. This effect describes that a mass m, which is in motion with the velocity v in a frame of reference, rotating at angular rate w, experiences a so called Coriolis force F_C:

$$F_C = -2m \cdot (w \times v) \tag{2.3}$$

The Coriolis effect can be quantified by measuring vibrating elements in the gyroscope. When the gyroscope is rotated, a vibration along the perpendicular sense axis is induced. The angular rate can be computed by measuring the secondary rotation of the vibrating mass [Woo02]. In electrical sensors the rotation is gauged using capacitive, piezoresistive or electrostatic approaches [Bao05]. The sensor's principle is illustrated in Figure 2.4.

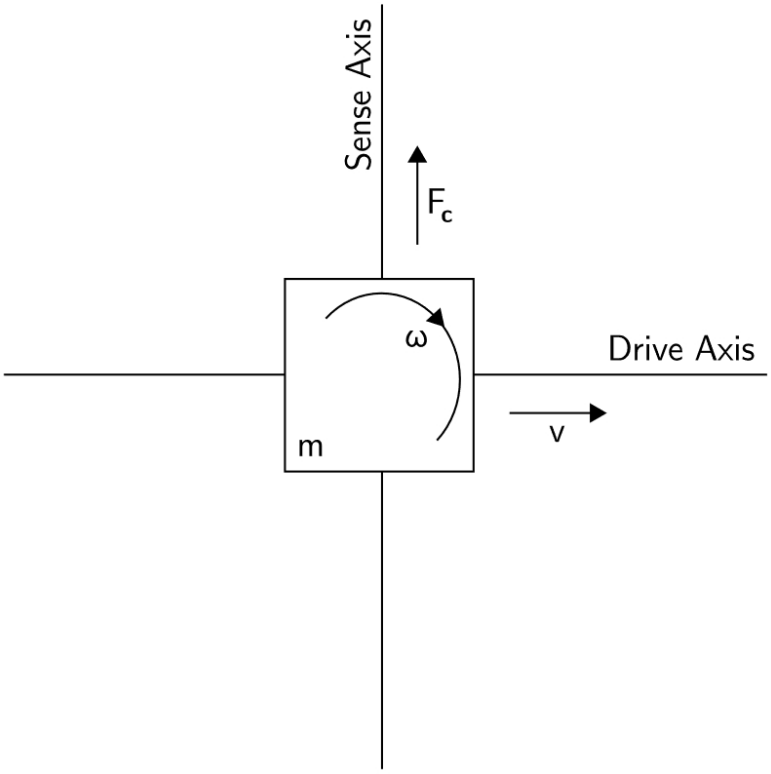

Figure 2.4: Vibrating Mass Gyroscope. A gyroscope measuring the angular rate w [Woo02].

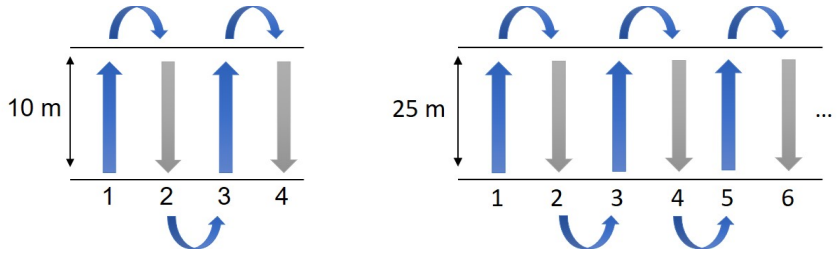

(a) 4x10m Test **(b)** Two Minute Walking Test

Figure 2.5: Two Gait Tests. Two specific tests for sensor-based assessment of gait.

2.2.4 Standardized Gait Tests

For calculating standardized rating scales subjects perform standardized gait tests. Their performance is evaluated subjectively by a clinician according to guidelines of rating scales (UPDRS motor score, H&Y). Different tests exist to investigate events like movement initation, turning sequences and stair-climbing.

Furthermore, there are gait tests developed for sensor-based gait analysis such as the 4x10m test, the two minute walk tests, timed-up-and-go test, stop-and-go test and heel-toe tapping, which are performed in gait laboratories. Motion is recorded with a sensor system like the inertial sensors. Resulting micro characteristics can support the expert with additional information in the form of gait parameters.

4x10m Gait Test

The subject walks 10 meters in a flat environment without any obstacles. After the first 10 meters, the subject turns around clock-wise and walks back to the starting point, turning again and repeating this procedure for a second time. This test should not include any pause [Ste08]. The focus is on the assessment of gait and especially the turning sequences of the subject [Bar17]. In Figure 2.5 the test is illustrated. Furthermore a typical IMU-ouput for all six resulting signals, recorded during a 4x10m test, is plotted in the Figure 2.6.

Two Minute Walking Test

The subject walks 25 meters in a flat environment without any obstacles back and forth for 2 minutes at a self-selected speed. Many turning sequences and intervals of straight gait occur in this test. The amount of covered distance differs and impaired subjects tend to lower speeds than healthy subjects [Sni07]. In Figure 2.5 the test is illustrated.

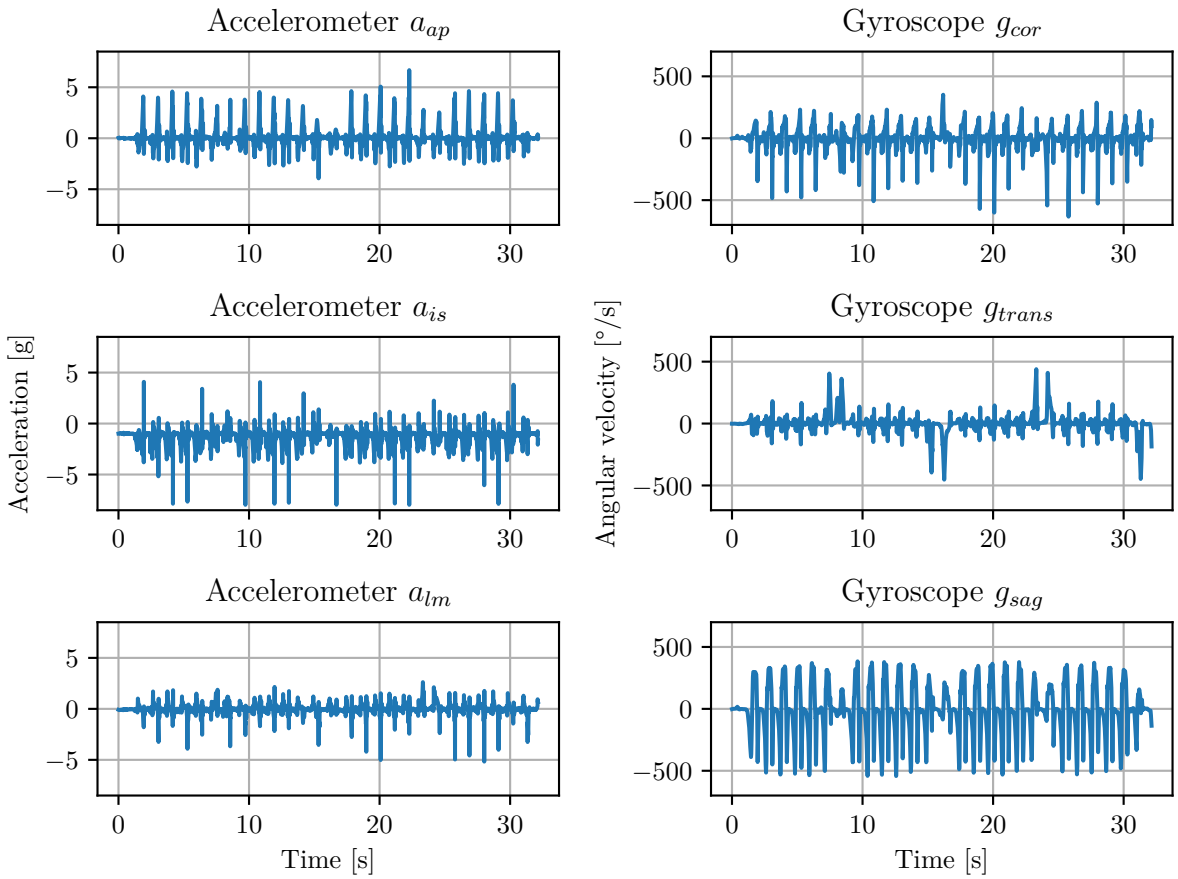

Figure 2.6: IMU-Recorded Gait Signals. All six resulting signals of an inertial sensor recording a four times 10 meter test. The turning steps after 10 meters of gait can be seen by the high peaks in the g_{trans}-signal and the low peaks in the g_{sag}-signal.

Chapter 3

Methods

At the beginning of this chapter the algorithm pipeline to detect clinical gait tests and calculate macro parameters is introduced. Figure 3.1 illustrates the methodlogy. The goal of this system is automatic detection of the specific gait tests 4x10m tests and two minute walking tests in recorded sensor data. Furthermore, macro parameters are calculated from WBs created with different MRP. To fit the home-monitoring dataset of the FallRiskPD project those steps are combined to one system.

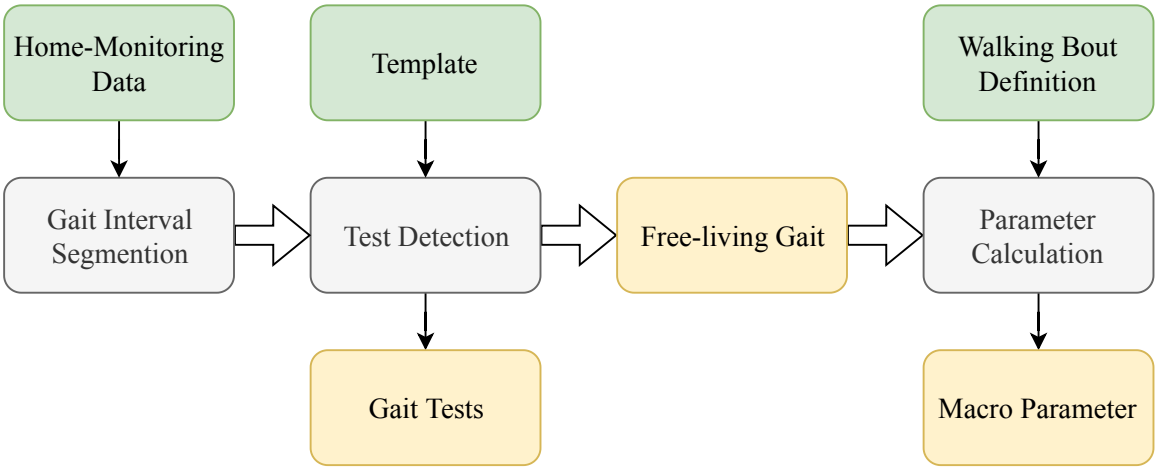

Figure 3.1: Algorithm Pipeline. The aim is to process home-monitoring data to detect gait tests and segmentate them from free-living gate. After segmentating intervals of gait, those intervals are processed to get relevant outcomes. By detecting gait tests, micro parameters during test performance can be computed. After dividing the home-monitoring data into detected gait tests and free-living gait, macro parameters can be calculated using a WB definition.

3.1 Gait Interval Segmentation

Before gait interval segmentation can be applied on sensor data, the raw data was preprocessed. For the data processing the raw sensor data was calibrated to correct the bias, scaling factors and physical orientation of the sensor. The sensor calibration developed by Ferraris et al was applied [Fer95].

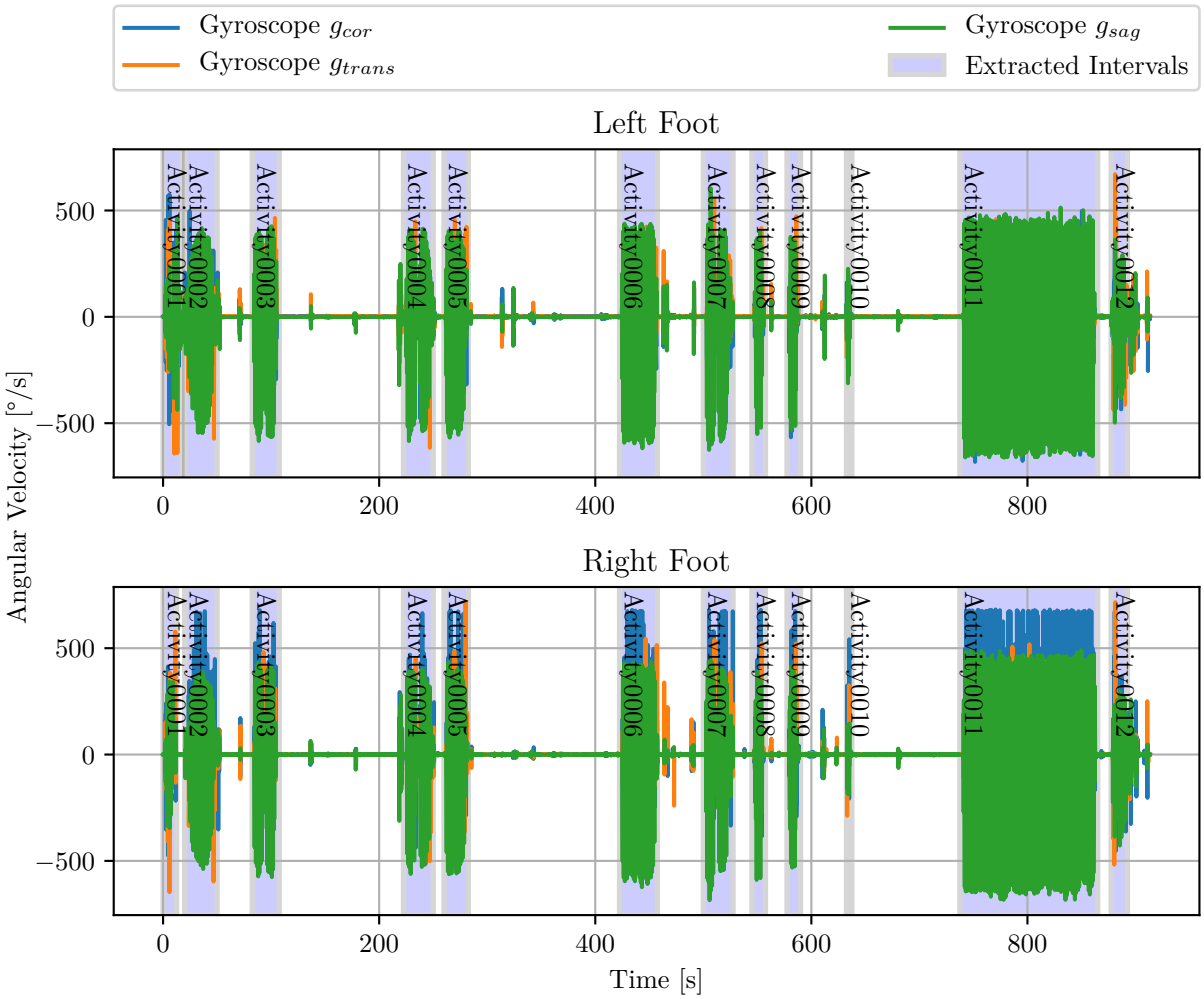

Figure 3.2: Gait Interval Segmentation. Possible result of the gait interval segmentation. Grey rectangulars represent intervals which were segmentated.

After the raw data is calibrated and aligned, segments of walking activity were detected in the data. This step will save calculation costs of the following processing steps by leaving out segments of rest and even more important, enabling the following test detection. For this reasons

sequences of activity were extracted.

The segmentation was performed with a sliding window algorithm, calculating a suitable measure of the area covered by the window. The algorithm was applied to the 3d-gyroscope g_{3d} and moving windows w had the length of 5 seconds. The overlap of consecutive windows was set to 50%. Assuming unsynchronized signals from left and right foot, the respective data was processed seperately.

Several steps were processed for each window w. First, windows which contained only rest and no activity were excluded. If the normalized signal magnitude area (SMA) of g_{3d}^{w} was exceeding a threshold set to 50 $^\circ/s$, the covered interval was taken into account for further processing [Kar06]. Those segments were assumed to contain walking activity. If overlapping or successive windows exceed the threshold, they were fused to one interval. The SMA is defined by the following equation, where g_{cor}, g_{trans} and g_{sag} are the gyroscope's signal in coronal, transverse and saggital plane:

$$SMA = \frac{1}{t}\left(\int_0^t |g_{cor}(t)|dt + \int_0^t |g_{trans}(t)|dt + \int_0^t |g_{sag}(t)|dt \right) \tag{3.1}$$

A exemplary output of this algorithm can be seen in Figure 3.2 showing the output of a 3d-gyroscope g_{3d} worn during a clinical session . As the segmentation is applied seperately to both feet output in both feet differs.

3.2 Gait Test Detection

In the following section an approach to detect standardized gait tests automatically is described. The tests detection is based on subsequent dynamic time warping (sDTW), a special form of dynamic time warping (DTW). As DTW algorithms are a form of template matching the generation of templates is also discussed in Section 3.2.2. Before applying the sDTW algorithm, the activity segments as well as the template have to be preprocessed. An explanation of this is found in Section 3.2.1. After peaks of the sDTW distance function have been determined, the possible gait test candidates get tested against several constraints, described in Section 3.2.3.

The basic concept of this detection algorithm is to create two sequences, template sequence and an input sequence segmentated by the gait interval segmentation, and measure similarity of the input to the template sequence. As similarity measure the sDTW distance cost is used. If the similarity is high enough we label the input sequence as detected gait test.

Considering the fact that human gait is a very complex movement pattern [Whi91], there is need to align template and input signal to obtain high similarity. Therefore different preprocessing steps to generalize input and template signal were made. The following assumptions were considered for the processing of template and test data:

- The 4x10m test and two minute walking test are made up of similar subsequences.
- This subsequence contains one segment of straight gait and turning steps after covering the requested length. One section of the 4x10m test is 10m and one section of the two minute walking test is 25m long.
- Each subject has an individual gait leading to different signal patterns.
- Different amount of steps are needed for one subsequence depending on the subject.
- For each turning sequence rotations in the transverse plane are performed.
- Those turning sequences produce peaks in the gyroscope's transverse plane.

The following preprocessing is based on these assumptions, especially the existance of turning sequences.

3.2.1 Signal Preprocessing

To achieve accurate outcomes, input sequences have to be preprocessed. This includes normalization, filtering, smoothing and squaring. Signals recorded by the 3d inertial sensor are continous movement sequenes $\mathbf{S}$ with the length N where $\mathbf{S} = (\mathbf{s_0}, ..., \mathbf{s_{N-1}})$. Each sample $\mathbf{s_n}$ of $\mathbf{S}$ with $n \in \{0, \ldots, N-1\}$ consists of data from accelerometer (a_{ap}, a_{is}, a_{lm}) and gyroscope $(g_{cor}, g_{tran}, g_{sag})$:

$$\mathbf{S} = (\mathbf{s_0} \ldots \mathbf{s_{N-1}}) = \begin{pmatrix} s_{ap,0} & s_{ap,1} & \cdots & s_{ap,N-1} \\ s_{is,0} & s_{is,1} & \cdots & s_{lm,N-1} \\ \vdots & \vdots & \ddots & \vdots \\ s_{sag,0} & s_{sag,1} & \cdots & s_{sag,N-1} \end{pmatrix} \tag{3.2}$$

For the detection algorithm only samples of the sequence $s_{trans,n}$ with $n \in \{0, ..., N-1\}$ of the gyroscope's transverse plane is used. For this reason the signal sequence $s_{trans}(n)$ was defined:

$$s_{trans}(n) = [s_{trans}(0), ..., s_{trans}(n-1)] \tag{3.3}$$

Figure 3.3 shows the workflow of preprocessing for two segementated intervals of activity. Both activities contain a 4x10m test. The goal of preprocessing is to align those two sequences to obtain high similarity and therefore low sDTW distance costs.

Normalization

To process data from sensors that differ in range, the input data was normalized to a numerical range of [-1; 1]. Normalization is done by dividing the transverse plane signal $\mathbf{s_{trans}}$ by the positive values of the sensor range of the gyroscope $g_{trans,range}$:

$$s_{trans,norm}(n) = \frac{s_{trans}(n)}{g_{trans,range}} \tag{3.4}$$

Filtering

The concept of filtering is to differentiate between different bands of frequencies. Filters are mostly classified by their frequency selectivity like lowpass, highpass and bandpass filters. Each filter can completely be defined by two sets of specifications, the frequency specifications describing the passband or stopband and the gain characteristic [The05]. For the test detection input signals are low-pass filtered with a butterworth filter of first order and cutoff frequency of 0.5 Hz. This frequency is the lower bound for the human "lokomotor" band [Bac10]. Thus, frequencies related to straight gait get suppressed. Afterwards the low frequency content of the repeating turning sequences is strongly prominent. For this step the Python (Python Software Foundation, Delaware, USA) functions *butter_lowpass* and *lfilter* were used for filtering signals. Equation 3.5 shows the formula for filtering the signal $s_{trans,filtered}$ by convolution with the impulse response $h_{butterworth}$ of a specific butterworth filter.

$$s_{trans,filtered}(n) = (s_{trans,norm} * h_{butterworth})(n) \tag{3.5}$$

Smoothing

One assumption for this algorithm was that each peak in the gyroscope's g_{trans}-axis signal is referring to one step. To diminish differences in the signal due to different amount of steps the signal was smoothed. On the one hand tall peaks which represent turning sequences should be preserved and fused to one peak as it is illustrated in (C) and (G) of Figure 3.3. On the other side small peaks representing straight steps should be erased. Therefore, a median filter was applied, as it preserves sharp changes [Ata81], referring to turning, and also removes impulsive content [Ata81], which are the straight stride's peaks. The median filter smooths the input by taking the median value of all sample values which are covered by the median filter's window size w. The signal $\tilde{s}(n)$ is defined as the signal $s(n)$ which lies within the interval $[-\frac{w}{2}; \frac{w}{2}]$ around the sample n. The window size w was set to 2 seconds. In the algorithm this processing was realized by the Python function *medfilt*. The function *median* in Equation 3.5 is performing the computation of the median value in the input sequence $\tilde{s}_{trans,filtered}$.

$$s_{trans,smoothed}(n) = median(\tilde{s}_{trans,filtered}(n)) \tag{3.6}$$

Squaring

The last step of preprocessing is squaring the signal point by point. This nonlinear amplification of the input signal intensifies the effect of the previous smoothing and filtering [Pan85]. Peaks of the turning sequence remain, while activity of straight gait hardly remains:

$$s_{trans,preprocessed}(n) = s_{trans,squared}(n) = [s_{trans,smoothed}(n)]^2 \tag{3.7}$$

The resulting signal after preprocessing is defined as $s_{trans,preprocessed}(n)$. For reasons of simplicity the index $trans$ and $preprocessed$ are ommited in the next sections although only preprocessed transverse-plane inputs are used for the following sDTW algorithm.

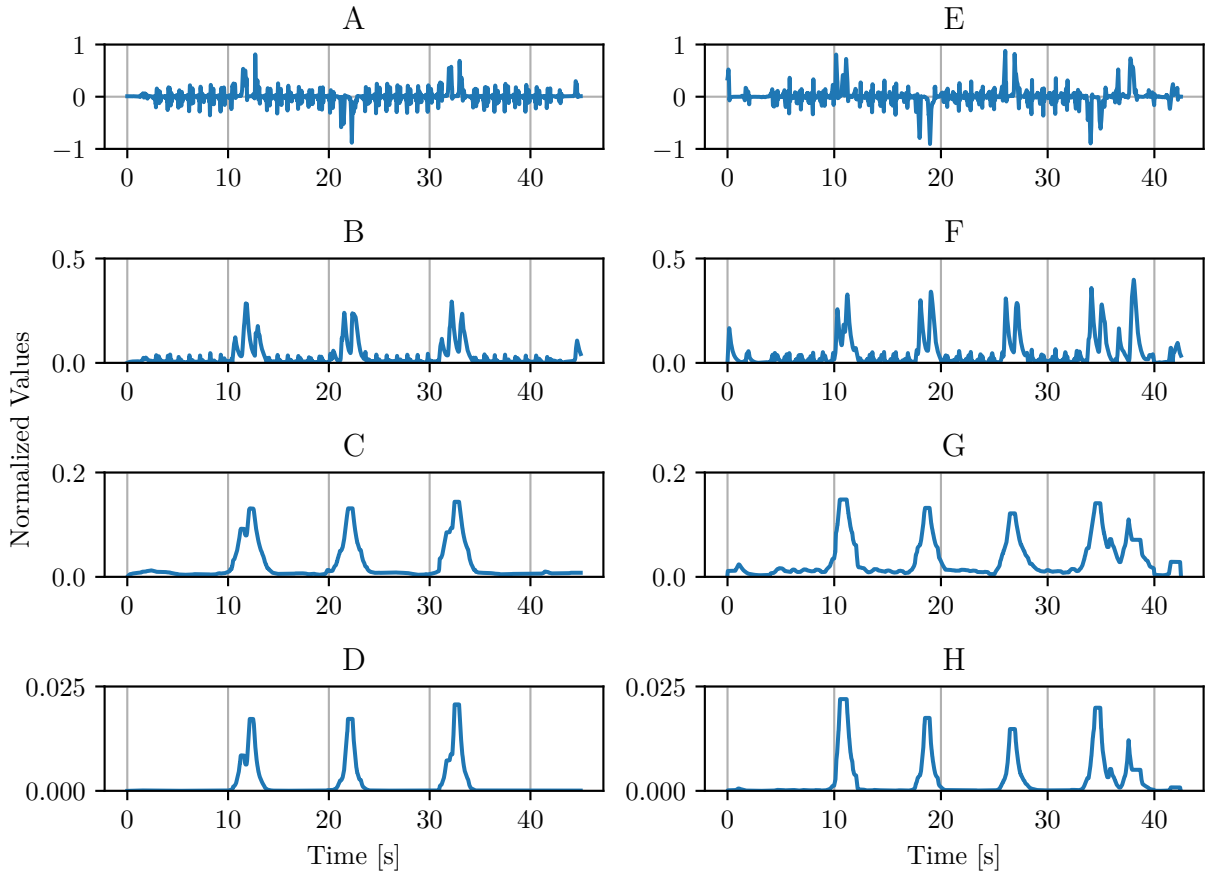

Figure 3.3: Preprocessing of Input Signals. This example shows the workflow to align two sequences which contain a 4x10m test. In (A) and (E) signals which are segmentated by the activity segmentation of section 3.1 are shown. Both signals are normalized to numerical values of [-1; 1]. Furthermore, in (E) there is activity in form of turning steps right after the test ends. As activity proceeds those steps are also added to the segment by the gait interval segmentation of Section 3.1. After normalization values of (A) and (E) get low-pass filtered and with taking the absolute value, outputs like (B) and (F) are created. Afterwards a median filter is applied to smooth the signal. Smoothed signals are (C) and (G). The last step is squaring the smoothed sequences. The preprocessed output signals (D) and (H) are containing the characteristic three peaks representing the turning sequences of the 4x10m test. The fourth and fifth peaks in (H) are resulting from additional activity after the end of the gait test.

3.2.2 Subsequent Dynamic Time Warping

DTW is used to indentify patterns that vary in time or speed by matching them nonlinearly [Mye81]. It is a template-matching approach with the benefit of being time invariant [Mül16] and can compute a similarity measure between two time series [Sil16]. One sequence is the test signal and the other one the input signal, possibly containing gait tests. By warping the template in the time domain an optimal fit between input and template is achieved [Bar17].

It is a commonly used technique for quantifying similarity and has been previously introduced to the field of gait analysis. One example is the work of Derawi et al. which extracted strides from subjects and compared them to refernce strides by DTW for user idenfication [Der10]. Another application is automatic stride segmentation which was developed by Barth et al. [Bar17].

In this work a special form of DTW algorithms is employed. The sDTW is used to find a subsequence of a continous signal sequence similar to a given reference pattern [Mül16].

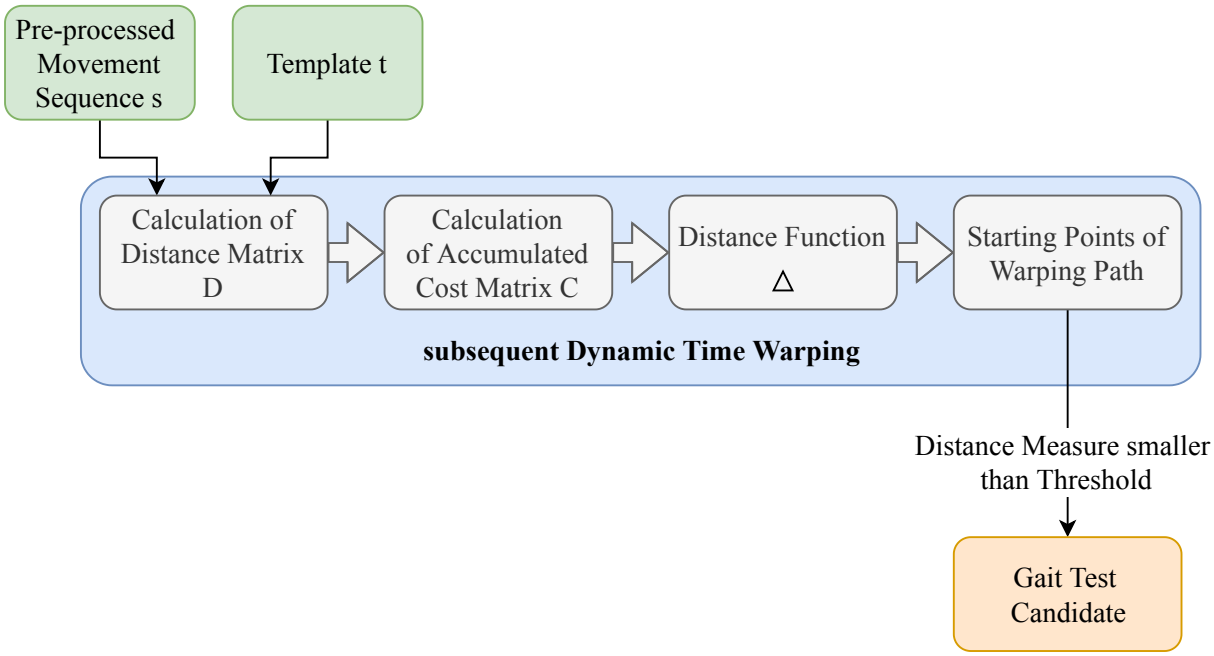

Figure 3.4: Template Matching Workflow. Workflow to measure similarity between movement sequence s and template t. After the sDTW algorithm is applied, a distance measure related to similarity between both input sequences is returned. If the distance measure is smaller than a predefined threshold θ the processed movement sequence is a candidate for gait tests and will be checked against postprocessing constraints of Section 3.2.3.

Template Generation

The template t_{trans} was created based on the assumptions made in section 3.2. Due to the fact that 4x10m tests and two minute walking tests are made up of similar subsequences the goal was to identify them by the same procedure simultaneously. A subsequence is a signal containing the interval of straight gait covering the whole track of 10m (4x10m test) or 25m (two minute walking test) and turning strides of the 180° turn around at the end of each segment.

As sDTW is time invariant, the different durations between turning sequences for the two tests can be neglected. Templates were generated from 4x10m tests transverse-signals. Since the pattern of the 4x10m test is contained in a two minute walking test, sDTW will also give in this case useable output values.

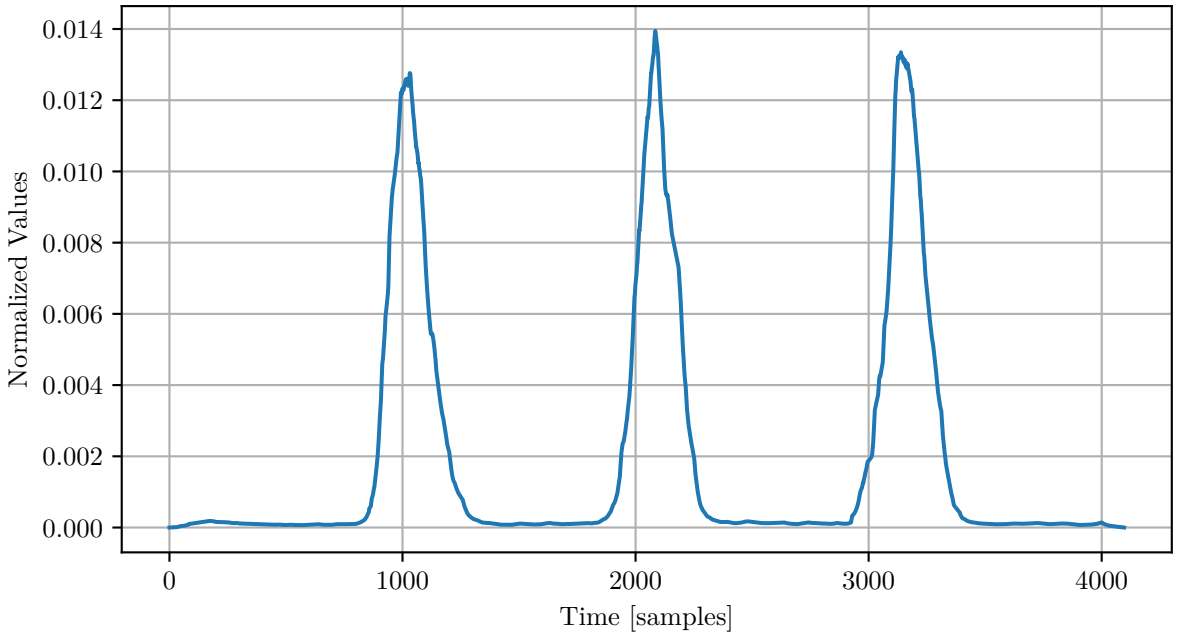

Figure 3.5: Generated Template. This is a template generated of 50 different 4x10m gait tests.

Furthermore, several signals were used and averaged to create a generalized template t. For this reason an additional resampling step was introduced to the preprocessing stage described in Section 3.2.1. Normalization, filtering, smoothing and squaring was applied with same parameters as for input signal preprocessing. The resampling was performed using the Python function *resample*. Figure 3.5 shows an example of a generated template from 50 manually labeled 4x10m tests. Only data of the left foot was used for this template.

Calculation of Distance Matrix

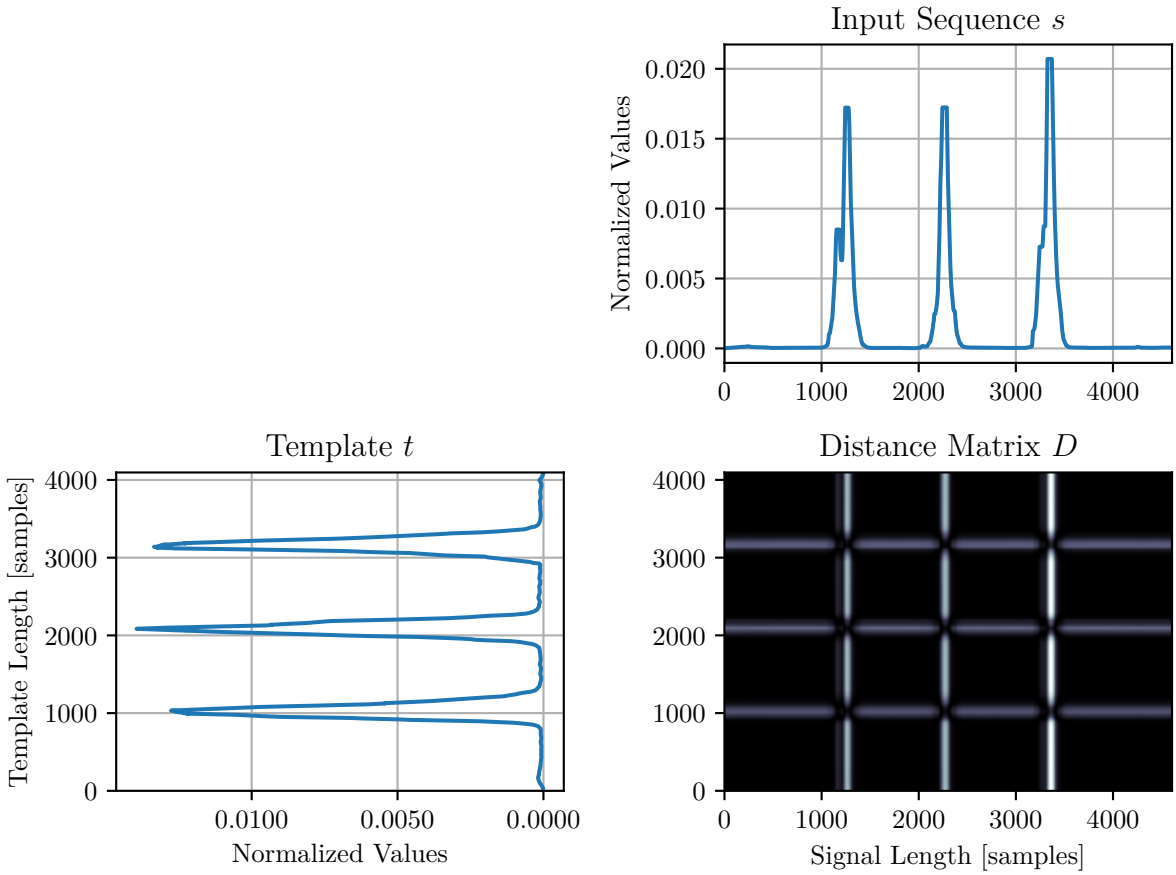

Figure 3.6: Calculation of Distance Matrix. Distance Matrix of template from Figure 3.5 and input sequence (D) from Figure 3.3.

The first process of the sDTW algorithm was to construct a distance matrix $\mathbf{D}$. It contains similarity measurements between the movement sequence s_{trans} and the template t sequence. The resulting matrix $\mathbf{D}$ is from the dimension $M \times N$, where M is the length of template t and N is the length of the input sequence s. For a sample point $t(n)$ the distance to a sample point $s(m)$ is calculated. This distance value is the value of the point (m, n) of the distance matrix $\mathbf{D}$. As distance norm the Euclidian norm is used. Each entry in the distance matrix $\mathbf{D}$ is defined as:

$$\mathbf{D}(m,n) = \sqrt{(t(m) - s(n))^2} \quad \forall\, m \in \{0, ..., M-1\}, n \in \{0, ..., N-1\} \tag{3.8}$$

If the local Euclidian distance $\sqrt{(t(m) - s(n))^2}$ is small, the similarity between both samples is high. The bottom row of the distance matrix $\mathbf{D}$ represents the distance between the first template sample $t(0)$ and every sample of the input sequence $s(n)$. While the top row shows the distances to $t(N-1)$ accordingly.

In Figure 3.6 an example of a distance matrix calculation was performed. Dark values in the matrix show small distances and thus a high similarity between sample $t(m)$ and sample $s(n)$. Bright values represent a higher distance and less similarity.

Calculation of Accumulated Cost Matrix

In the accumulated cost matrix $\mathbf{C}$ the sum of distances between template and movement sequence and the accumulated costs of warping the template t to parts of the movement sequence s is represented. The accumulated cost matrix has the same dimensions as the distance matrix $\mathbf{D}$. The bottom row of $\mathbf{C}$ is filled with the values of the bottom row of distance matrix $\mathbf{D}$, as there is no warping for the first sample of t. From this row the cost matrix $\mathbf{C}$ can be filled.

$$\mathbf{C}(0, n) = \mathbf{D}(0, n) \; \forall \, n \in \{0, ..., N-1\} \tag{3.9}$$

The first column of $\mathbf{C}$ is computed by summing up all values from bottom to the current sample n of the first column of the distance matrix $\mathbf{D}$. Each sample of the first column $\mathbf{C}(m, 0)$ is initialized by the following equation.

$$\mathbf{C}(m, 0) = \sum_{i=0}^{m} \mathbf{D}(i, 0) \; \forall \, m \in \{0, ..., M-1\} \tag{3.10}$$

All remaining samples of $\mathbf{C}$ are calculated recursively. The element $\mathbf{C}(m, n)$ is the sum of the respective element $\mathbf{D}(m, n)$ and a cost element of a continuity condition which defines local constraints. For this, different step size conditions are used in literature [Mül10]. Therefore, in this algorithm only samples left, below and left below of $\mathbf{C}(m, n)$ are investigated to search the minimum warping costs. The accumulated cost matrix has to be filled from left bottom to right top of the matrix, while accumulated costs only include minimal costs.

$$\mathbf{C}(m,n) = min\{\mathbf{C}(m-1,n-1), \mathbf{C}(m-1,n), \mathbf{C}(m,n-1)\} + \mathbf{D}(m,n) \\ \forall\, m \in \{0,...,M-1\}, n \in \{0,...,N-1\} \tag{3.11}$$

The step size condition used in this work is plotted in Figure 3.7, which illustrates the calculation of one sample $\mathbf{C}(m,n)$ of the accumulated Cost Matrix by Formula 3.11.

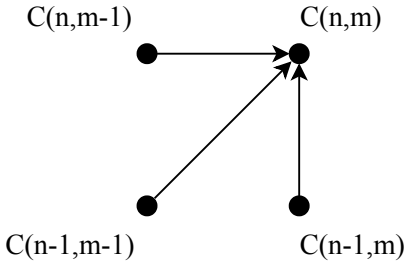

Figure 3.7: Step Size Condition. Cost matrix elements can be computed with this step size condition.

This recursive procedure has to be performed row by row. Therefore the top row of the accumulated cost matrix $\mathbf{C}$ represents the accumulated costs of warping t to s. An example of the distance matrix $\mathbf{D}$ and the respective accumulate cost matrix $\mathbf{C}$ is visualized in Figure 3.8. The distance matrix is identical with the matrix from Figure 3.6. Outgoing from the distance matrix a accumulated cost matrix can be computed.

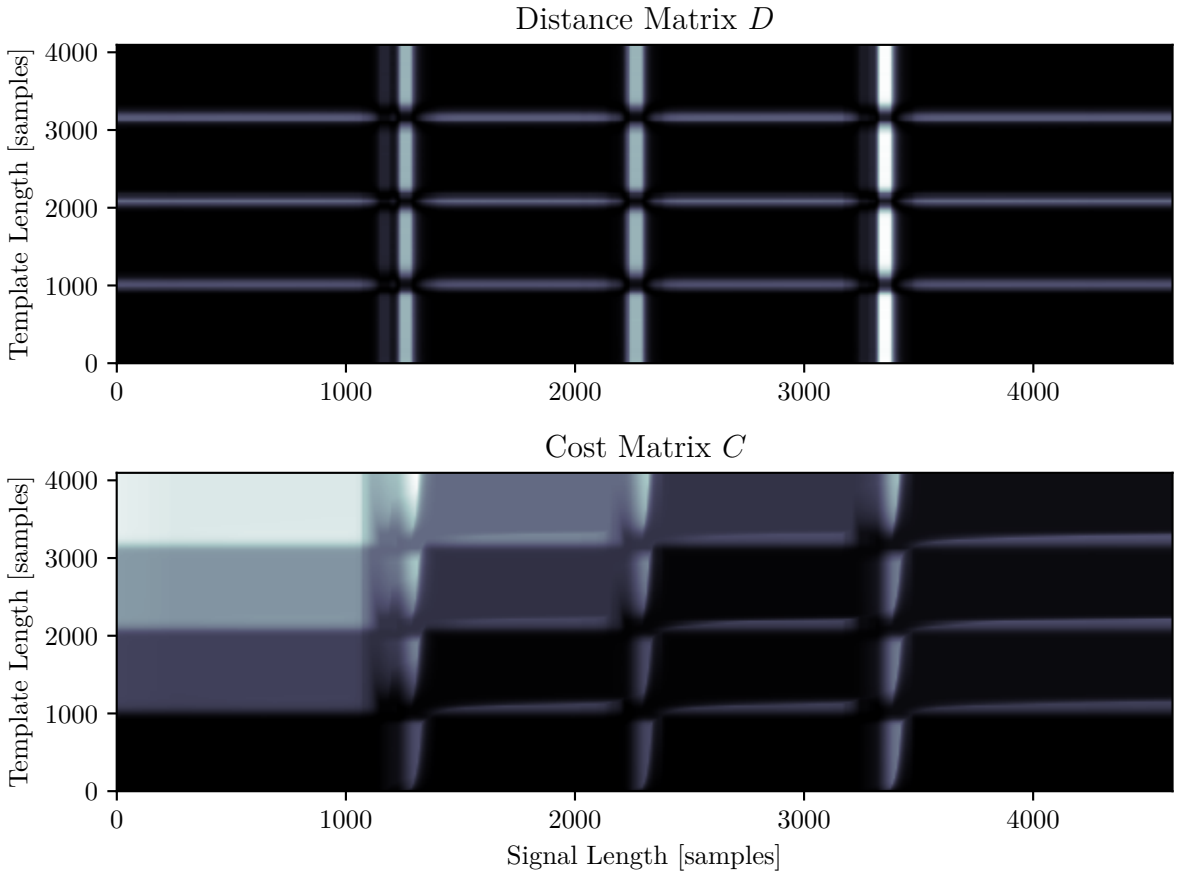

Figure 3.8: Calculation of Accumulated Cost Matrix. Accumulated cost Matrix computed with C template t from Figure 3.5 and input sequence s. The signal s is signal (D) from Figure 3.3. Dark samples represent low cost, bright samples represent high cost for warping the template t to the input signal s.

Distance Function

The top row of the accumulated cost matrix C represents the accumulated costs for warping the template t to the input signal s. The warping costs for the last sample of the template sequence, which is the end of the template's gait test, are in the top row of the cost matrix C. As this row represents the accumulated minimal warping costs, it is also called the distance function δ. To find cheap alignments of template to the input signal, local minima of the top row have to be found and are used as starting points p_0 for warping [Mül16]. In Figure 3.9 the distance function of cost matrix of Figure 3.8 is displayed.

$$\Delta(n) = \mathbf{C}(M-1, n) \, \forall \, n \in \{0, ..., N-1\} \tag{3.12}$$

Local minima from Δ are possible starting points for low cost warping with the sDTW costs of $\Delta(n)$. Low values of $\Delta(n)$ signalize low cost and therefore a high similarity. In this algorithm only the global minimum of Δ was compared to a threshold θ, since one assumption was that only one gait test was contained in the segmentated sequence, which was the input signal of the sDTW algorithm. If the value of sDTW distance function $\Delta(n)$ was less than the threshold θ the input signal was a gait test candidate. The minima were computed by the Python function *find_peaks*.

For 4x10m tests this distance function will have at least three local minima as there a three proposed turning sequences contained in the test. In the two minute walking test the amount of local minima changes from subject to subject. By checking if the sDTW distance is less than the threshold one can tell if the input is a gait test or is no gait test. Wheter the gait test is a 4x10m test or a two minute walking test needs additional postprocessing in this implementation, described in Section 3.2.3. As start and end of the gait test the respective start and end of the segmentated gait interval was used.

An example of identifying a 4x10m test is illustrated in Figure 3.9. For detecting a gait test first the global minimum of the distance function Δ is computed. If this minimum is lower than the predefined threshold θ the current input sequence is recognized as a gait test. The threshold θ was set to 0.015. Input is sequence (A) from Figure 3.3 and template from Figure 3.5. Figure 3.10 represents a detection of a two minute walking test. More turning sequences can be seen in the distance function. The cheapest warping path can cover each subsequence of three turning sequences in the two minute walking test.

Warping Paths

For this algorithm there is no need for computing the warping path, which is usually the next step for DTW. The template t is warped by the warping path for alignment to the input signal s. With this path the start of the first turning sequence included in the optimal warping path could be computed. Due to the fact that the sDTW cuts off the segments of rest on the outer parts, right of the last turning sequence or left of the first turning sequence, a different approach was used. Further problems would have been occured with the two minute walking test. Asigning the whole segmentated gait interval was found to be a good alternative. For sake of lucidity the warping paths are plotted in Figure 3.9 and Figure 3.10. An explanation for warping path calculation can

be found in the work of Müller et al. [Mül16].

After applying the sDTW algorithm the segments which sDTW distance are less than the predefined threshold θ are checked for several constraints, described in the following postprocessing section.

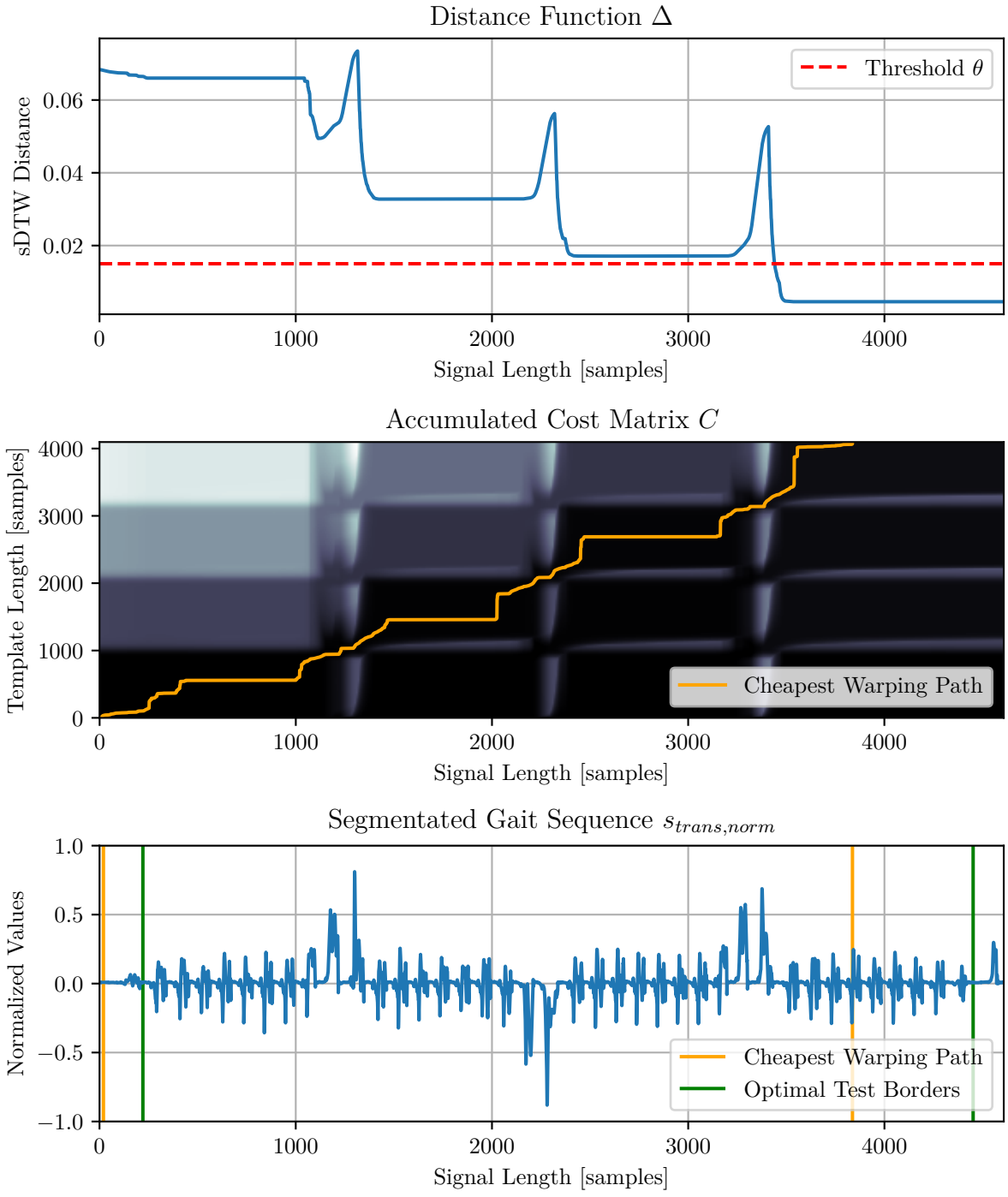

Figure 3.9: Calculation of Warping Path 4x10m Test. This graphs represents the detection of a 4x10m test. By observing the global minima of the distance function Δ the decision wheter it is recognized as a gait test or not was made.

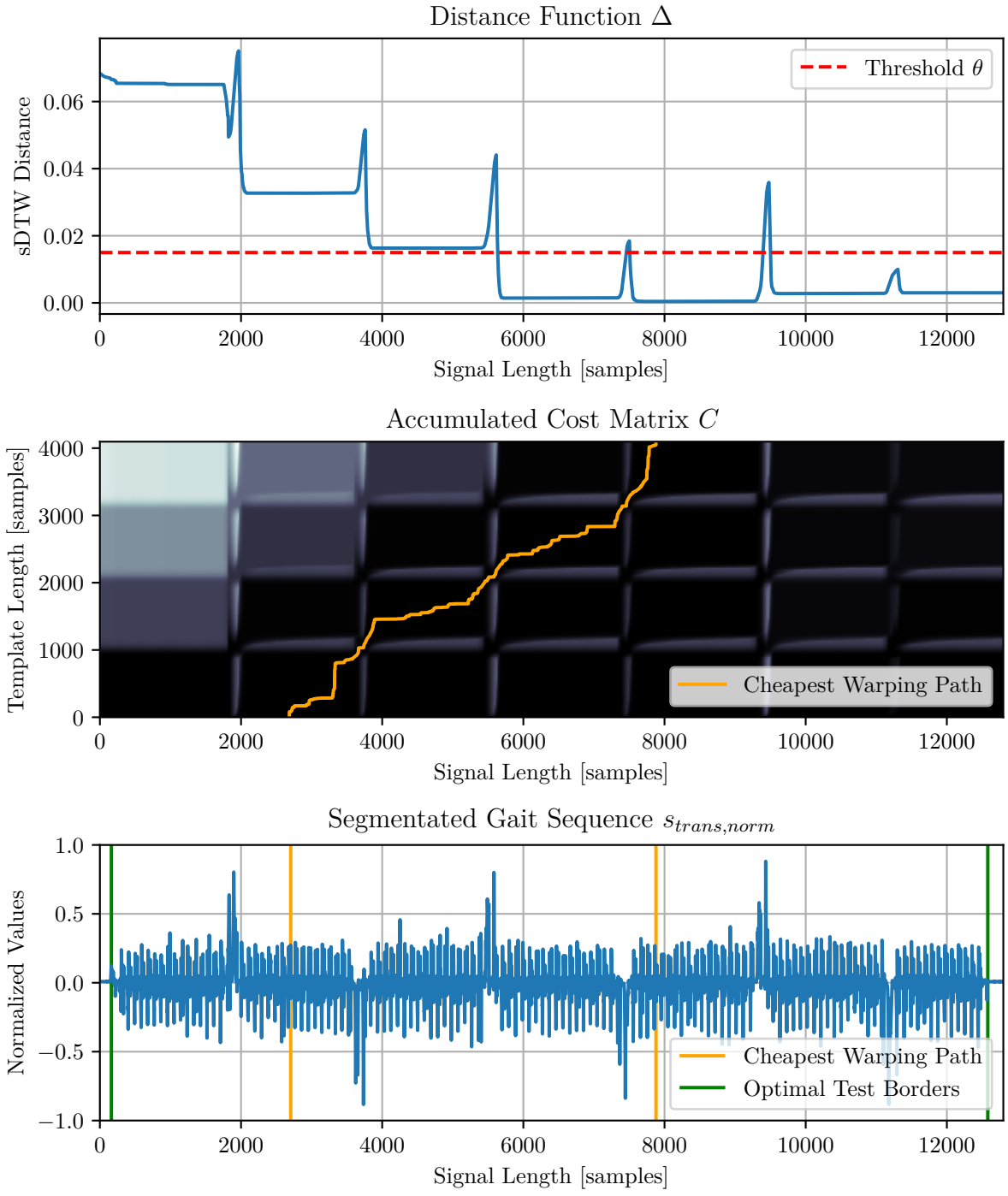

Figure 3.10: Calculation of Warping Path two Minute Walking Test. This graphs represents the detection of a two minute walking test. By observing the global minima of the distance function Δ the decision wheter it is or is not a gait test is made. The cheapest warping path covers the best fitting three turning sequences.

3.2.3 Postprocessing

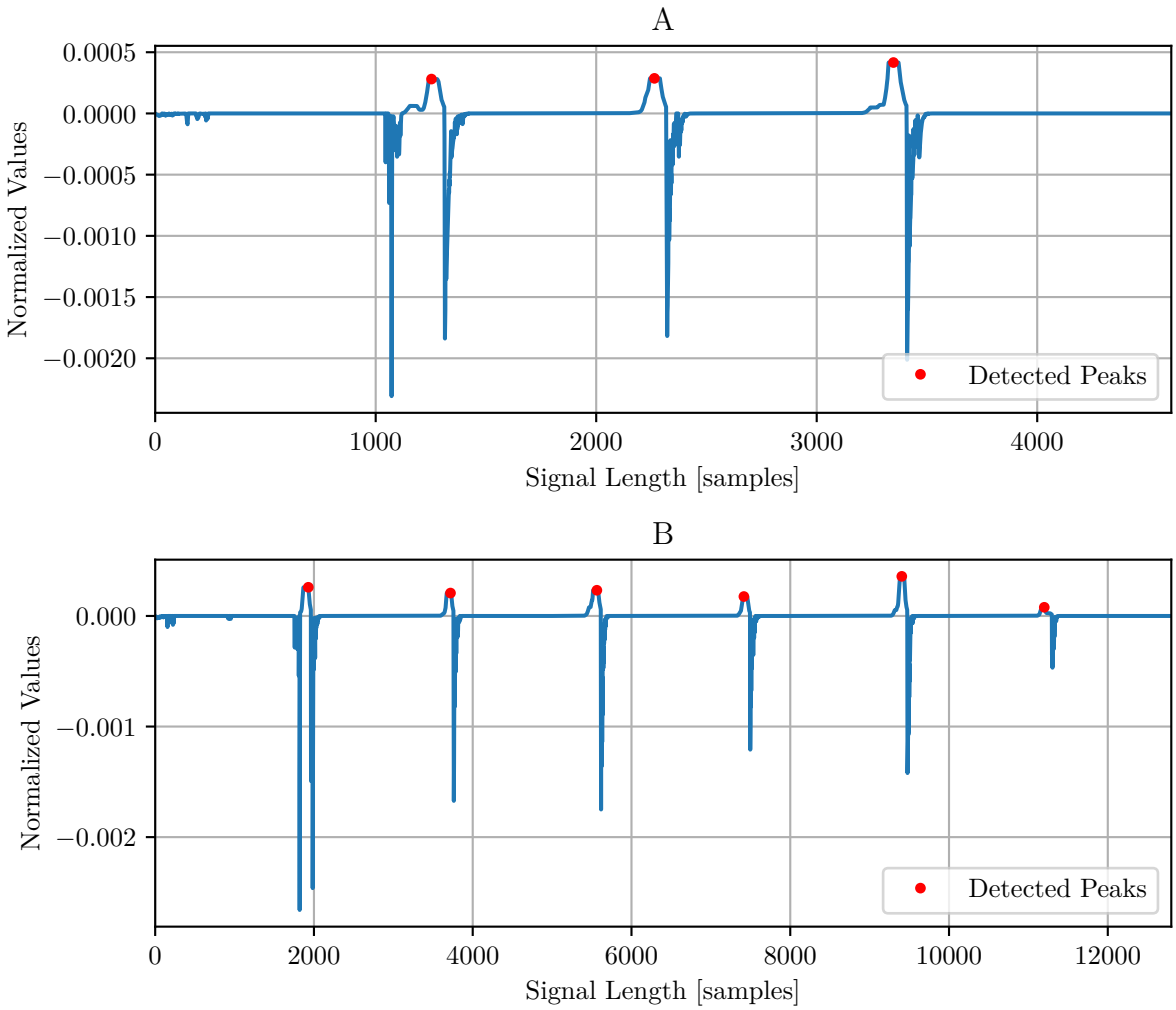

Figure 3.11: Counting of Turning Sequences. In (A) three peaks were detected, while in (B) six peaks were detected. Amount of turning sequences was found to be a good discriminating feature between free gait, 4x10m tests and two minute walking tests for the segmentated intervals.

After possible gait tests were detected, they were observed for some constraints. By checking the amount of turning sequences test candidates were classified into 4x10m tests and two minute walking tests. Each turning sequence lead to an local maxima in the distance function Δ, hence the distance function was used to count turnings in the test candidates

If the candidate contained three turning sequences then it was recognized as a 4x10m test. Due to the fact that after performance of gait tests, there was often turning activity also four peaks in

the distance function were accepted as 4x10m tests. Furthermore the amount of strides of a single foot contained in the candidate's segment had to exceed 18 steps. This value is the average value minus the double standard deviation of all 4x10m tests contained in the template creation data set of Figure 4.2, introduced in Section 4.2. Strides were segmentated with the sDTW algorithm of the stride segmentation of Barth [Bar17] without any stride constraints.

On the other hand for classifying candidates as two minute walking tests, there was no fixed amount of turning sequences, but a defined amount of time. Therefore the candidates which lasted from 110 seconds to 180 seconds and contain more than three turning sequences were labeled as two minute walking tests. Also there was a lot of turning activity after the test ends, which was the cause to set the maximum time to 180 seconds.

Turning sequences were identified by searching for peaks in the first deviation of distance function Δ. For this the Python function *gradient* was used. This deviation was observed for maxima with *find_peaks*, where distance between successive peaks had to exceed 650 samples and the peaks values had to be at least 5 % of the maximum peak to erase peaks due to noise. In Figure 3.11 (A) the deviation of the distance function Δ from a segment containing a 4x10m test is seen. Three turning sequences were detected. In Figure 3.11 (B) a two minute walking test with six turning sequences was detected. An examplary output of the test detection is illustrated in Figure B.2.

Since gait tests can be detected automatically ,further the data can be divided into gait tests and free gait. Another important aspect of analyzing home-monitoring data is calculation of macro parameters, which are computed on free-living gait data. The next section is covering this topic.

3.3 Macro Parameter Calculation

To generate clinically relevant outcomes, calculation of macro parameters was performed. Macro parameters quantify broader trends of gait observed over long time [Del17]. These parameters describe relations between WBs like volume, pattern and variability of those WB.

3.3.1 Walking Bout Definition

For comparing different WB definitions and their effect on the outcome parameters two definitions from literature were used. The first definition is originally from Del Din et al [Del17]. They set the MRP to 2.5 seconds and a minimum amount of three steps. The second WB definition had also a minimum of three steps, but a MRP of ten seconds and was used by Orendurff [Ore08].

3.3.2 Calculation Of Parameters

As macro parameters were calculated from WBs, firstly WB had to be generated from the gait intervals, segmentated by the method of Section 3.1. A WB definition was used to compute WB from those intervals. This was done by a sDTW based single straight stride detection algorithm developed by Barth, which returns all strides detected by the sDTW, which do not exceed a specific threshold optimized for PD patients [Bar17]. Afterwards a event detection algorithm was applied which is partly based on the works of Rampp et al. [Ram14]. Each detected stride was observed. If time between stride end, which was a MS event, and stride start, the previous MS event, did not exceeded the respective MRP given in Section 3.3.1, those strides were fused to a list. Those MS events were calculated with the method of Skog et al. [Sko10]. If the amount of strides in this list were higher than two strides, a WB was generated, which lasts from the list's first stride's start to last stride's end.

With these WB generation, calculation of different macro parameters were performed. The set of macro parameters observing each day contained *number of steps* per day, *number of WBs* per day and the *mean WB length*. Furthermore macro parameters based on the total number of WBs of all days were calculated, which were frequency of WB with different WB durations and frequncy of WBs with different numbers of *steps in a row*.

Chapter 4

Experiments

In this chapter the used data sets are introduced. Due to a lack of sufficient home-monitoring data, the gait test detection algorithm was trained and tested on test sessions in a clinical environment. For the calculation of macro parameters another small home-monitoring data set was used.

4.1 Gait Test Detection

To improve the results of the gait test detection, optimization of detection related parameters, especially the generation of templates and the optimal threshold for the sDTW distance, were performed.

Figure 4.1: Shimmer 2R Sensor. IMU-sensors attached to the shoe and all the signals which are recorded by accelerometer (A) and gyroscope (G) [Bar17].

4.1.1 Study Design

For training and testing the gait test detection algorithm, there was a data set of patients with idiopahtic PD, which was aquiered at the movement disorder outpatient unit of the University Hospital Erlangen. As sensors they used Shimmer 2R (Shimmer Sensing, Dublin, Ireland), inertial sensor units (*IMU*), which were attached on the lateral side of the shoes. In Figure 4.1 this attachment is illustrated. The sensor's recording rate was 102.4 Hz and the IMUs consist of a 3-d accelerometer (range $\pm$ 6g) and a 3-d gyroscope (range $\pm$ 500 °/s).

Table 4.1: Subject Characteristics

Age [years]	63.0 $\pm$ 10.8
Height [cm]	171.2 $\pm$ 15.8
Weight [kg]	78.8 $\pm$ 16.5
UPDRS motorscore	17.6 $\pm$ 9.6
H&Y	2.2 $\pm$ 0.8
Sex (m/f)	106 / 63

The data was recorded during clinical gait sessions, while the subjects performed different batteries of gait and movement tests. Gait tests included: 4x10 meter test at self-preferred speed, two minute walking tests, two times 10 meter test with and without dual task, 10 meter obstacle steps, timed up and go test and two times 10 meters stop and go. Movement test included: heel-toe tapping, sit to stand transition and stand on one leg. The tests were performed in a clinical setting and observed by a physician. The subjects performed the battery of tests, while the physician set time stamp annotations for the sensor data manually. Those labels contain the test type and start and stop of the specific test. Between different tests there were short resting times. One resulting data set is shown in Figure B.1.

To gain high generalisation, different hyperparameters of the test detection were optimized seperately with different data sets. Figure 4.2 shows the splitting of data sets, which is used to suppress overfitting.

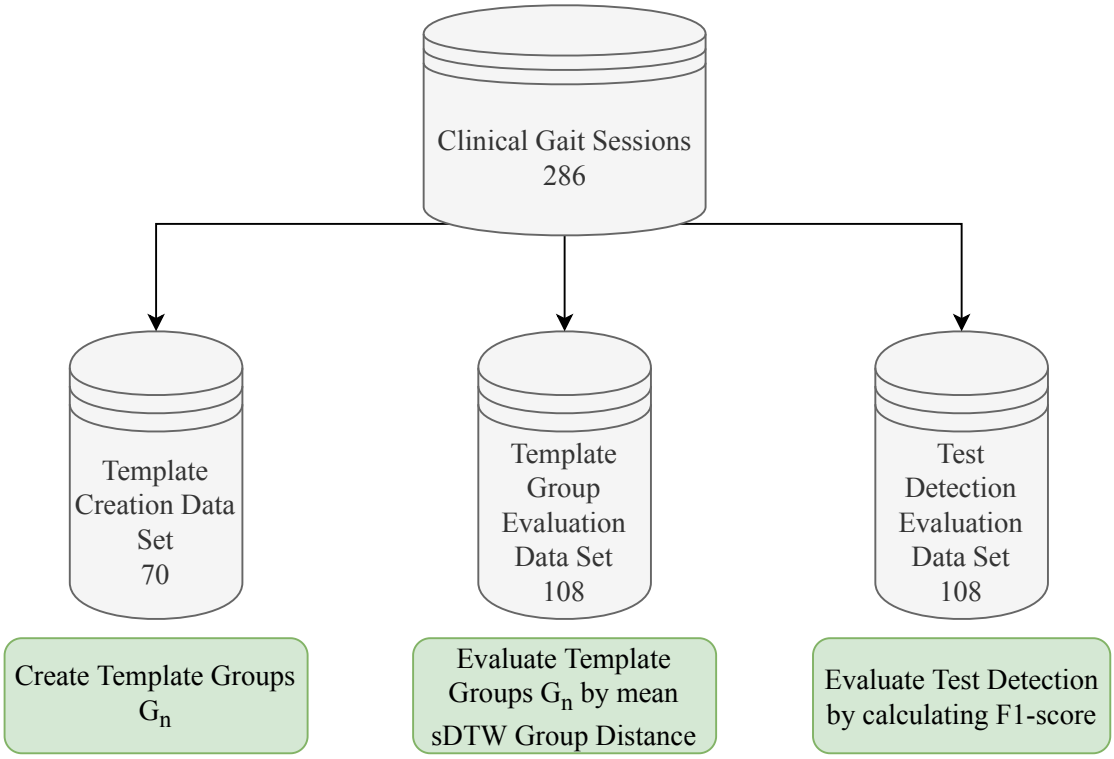

Figure 4.2: Data Set Split. The available data of 286 clinical gait sessions was splitted in three data sets, each for a different optimization matter.

4.1.2 Template Creation

Optimizing the template was one parameter to improve the outcome results. It was assumed that the sDTW distance is the quality measure for templates, small values represent high similarity and therefore good quality. If the sum of all sDTW distances of one single template to each gait test of a list was small, the template was considered to be good. A small value of the summed up sDTW distances signals, signals that the template is similar to the average input signals.

For this reason, two different data sets were used, one from which templates were created and another to evaluate the templates with the sDTW distance. To obtain general outputs an optimal number of sequences used for template creation had to be found. Therefore, six template groups, each group containing templates generated from the same number of test sequences, were defined. Templates were created like described in Section 3.2.2. The sequences which were taken for template generation are 70 different 4x10m tests from the template creation data set which is shown in Figure 4.2. For accurate template generation, the template creation data set was labeled manually by the author.

Every template group contained 20 different templates. Each template of one group was generated with the same amount of test sequences, where the number of test sets used for one template generation are j and $j \in \{2, 5, 10, 20, 50, 60\}$. Each group is refered as G_2, G_5, G_{10}, G_{20}, G_{50} and G_{60} and each group contains templates $t_{j,1}$, $t_{j,2}$,...,$t_{j,20}$. So group G_2 contains the templates $t_{2,1}$, $t_{2,2}$,...,$t_{2,20}$.

To create one template, the respective amount of already preprocessed test signals was summed up and divided by the amount of test signals used for creation. Each test signal was preprocessed, which consisted of normalization, filtering, smoothing and squaring. This was the same process as for an input sequence for sDTW computing described in Section 3.2.1. Furthermore all templates were resampled to 4096 samples, while the mean 4x10m test length of the 70 template creation test sets is 3800 samples. Only data from the left foot was taken into account to create the template. The averaged template is now refered to as $t_{j,m}$, with $m \in \{0, 1, ..., 20\}$ and for each of the 20 templates, a set of j randomly chosen test sets of the 70 test creation data set were taken.

To obtain the sDTW performance of each group G_j, with $j \in \{2, 5, 10, 20, 50, 60\}$ the mean of sDTW distances to a test set was computed. For a template $t_{j,m}$ the sDTW distance to all input segments s of a list S was calculated. A list contains the 108 manually labeled 4x10m gait tests of the template group evaluation data set of Figure 4.2. Those 108 distance values were then averaged to the value $d_{j,m}$. This was done for each template $t_{j,m}$ of every group G_j.

These averages of sDTW distance measures $d_{j,m}$ were used to calculate an average group distance measure $\bar{d}_j$, which is assumed to quantify the overall test detection performance of the group G_j. The group G_j with the lowest sDTW mean of all groups is now refered as G_{opt}. A Welch-test were computed for the mean sDTW distances to observe if the mean of each group differs significantly between template groups G_j. The group with the lowest number of test sets used for template creation and the lowest mean sDTW distances after which no significant changes of the distance occur, was asigned as the template group G_{opt}.

4.1.3 Performance Assessment

As performance assessment for threshold adjustment of the maximal permissible sDTW distance between template t and input sequence s, the F1-score was applied. The threshold θ was introduced in Section 3.2.2. Maximizing the F1-score, by adjusting the threshold θ two aims are satisfied. Minimizing the number of missed tests, while keeping the amount of falsely detected segments as low as possible. The F1-score is calculated from precision and recall value. A high precision 4.2 represents that the ratio of detected tests to falsely detected free-living gait segments is high. On the other hand a high recall value 4.3 means that only few gait tests are omitted. The F1-measure

4.1 is the harmonic mean of precision and recall, where missed gait tests and wrongly detected gait tests are taken equally into account:

$$F1\text{-}score = 2 \cdot \frac{precision \cdot recall}{precision + recall} \tag{4.1}$$

The detection positives are the gait intervals, which were recognized as gait tests by the detection algorithm. Whereas the true positives are all detected intervals, which are also real gait tests in the gold standard data. Thus, if the precision is equal to one if all detected gait tests are 4x10m tests and two minute walking tests.

$$precision = \frac{\sum true\ positives}{\sum detection\ positives} \tag{4.2}$$

On the other hand, the recall or sensitivity value gives information on how many contained gait test were not recognized by the algorithm. The false negatives are those missed tests. If the recall is equal to one no gait test was missed. The following equation is the defintion of the recall value:

$$recall = \frac{\sum true\ positives}{\sum true\ positives + \sum false\ negatives} \tag{4.3}$$

4.1.4 Threshold Adjustment

The threshold parameter θ, introcuded in Subsection 3.2.2 for checking the sDTW distance measure, was trained to distinct between free-living gait and gait tests using the generated optimal template t_{opt}.

The test detection evaluation data set consisting of 108 manually labeled clinical sessions, each containing one 4x10m test and one two minute walking test besides some other motion tests was used for threshold adjustment. The data set is shown in Figure 4.2.

Results of the gait test detection were compared to ground thruth labels set by the physicans. If the borders of the detectioned test labels were within 15 seconds (4x10m test) or 60 seconds (two minute walking test) from the manual labeled test borders, the gait test was recognized correctly.

To optimize the threshold θ a 5-fold cross-validation was applied. Cross-Validation is a popular method estimating the accurancy of a classifier and adjusting hyperparamters to obtain outcomes of high generality [Koh01]. For each fold the threshold θ is trained on one fold's data, while the other folds are held out.

Therefore, the threshold is linearly increased in range of 0.001 to 0.033 in steps of 0.004. The threshold which led to the highest F1-score is the optimized threshold θ_{fold}.

After optimization on the single fold, the F1-score was calculated for the computed threshold θ_{fold} for all four held out folds. This was done for each fold seperately generating five thresholds. The mostly occured threshold θ_{fold} is the optimal threshold θ_{opt}.

4.2 Macro Parameter Calculation

For the calculation of macro parameters a data set of 11 recorded day, screening one single PD patient was used. The patient wore the mobile GaitLab system (Portabiles HealthCare Technologies GmbH, Erlangen, Germany) for different durations (time = 5.5 $\pm$ 1.7 hours)in his home environment. The IMUs were integrated in the midsole of special shoes. Figure 4.3 shoes the sensors used for home-monitoring. Their recording rate was 99.9 Hz and the IMUs consist of a 3-d accelerometer (range $\pm$ 8g) and a 3-d gyroscope (range $\pm$ 1000 °/s).

Table 4.2: Subject Characteristics

Age [years]	77
Height [cm]	182
Weight [kg]	83
UPDRS motorscore	31
H&Y	2.5
Sex (m/f)	1 / 0

In this study the subject was instructed to do test battery in their home environment. One test battery consists of three 4x10 meter tests, one at preferred speed, one at slow speed and one at fast speed.

Figure 4.3: Mipod Sensors. These are the sensors which were used for home-monitoring recording. They are integrated in the sole of shoes.

In the given data set only one sensor worked accurately, the following macro parameter analysis is based only on right foot data. Hence, the WB definition of Del Din et al. [Del17] had to be adapted to single foot data. The following assumptions, regarding counting steps from single foot data were made from Orendurff et al. [Ore08]:

$$steps = (2 \cdot right\ foot\ strides) \pm 1 \tag{4.4}$$

Therefore, detection of 2 single, right or left, foot strides are 4 ± 1 steps. For this thesis right foot data was observed:

- Left, Right, Left, Right, Left = 2 detected right foot strides = 5 steps
- Left, Right, Left, Right, or Right, Left, Right, Left = 2 detected right foot strides = 4 steps
- Right, Left, Right = 2 detected right foot strides = 3 steps

As home-monitoring data of consists of gait tests and free-living gait, the data has to be devided. WBs which are containing a detected gait test were left out. Therefore, the free-living gait WBs remain.

Chapter 5

Results

In the following chapter the results of the gait test detection algorithm and macro parameter outcomes are presented.

5.1 Gait Test Detection

For optimization of the test detection, template creation and threshold adjusting were performed, which is shown in the next sections.

5.1.1 Template Creation

As described in Section 4.1.2, an evaluation of template groups G_j was made, which differ in the amount of used test sets, which were averaged for the creation of templates. The mean sDTW distance for each template $t_{j,m}$ introduced in Section 4.1.2 was plotted in Figure 5.1 for each template group G_j.

Results of the Welch-test showed that only group G_2 shows significant differences for the mean of sDTW distances to all other groups. Also group G_2 has a much higher variance, while the standard deviation is sinking for higher numbers of tests used for template generation. Standard deviation of group G_5 was contrarily lower than of group G_{10}. The mean distance values of group G_2 are the highest ($d_{max} = 0.0366$) and also the lowest ($d_{min} = 0.0041$), also leading to the highest value of standard deviation ($SD_2 = 0.0082$). The lowest mean of the group sDTW distances was $\bar{d}_{60} = 0.0055$ of group G_{60}, while group G_{50} had the lowest standard deviation with $SD_{50} = 0.0001$.

Group G_5 was asigned to be the optimal template group G_{opt}, as it has a lower group mean

sDTW distance and groups with higher numbers of test sets used for template generation show no significant difference.

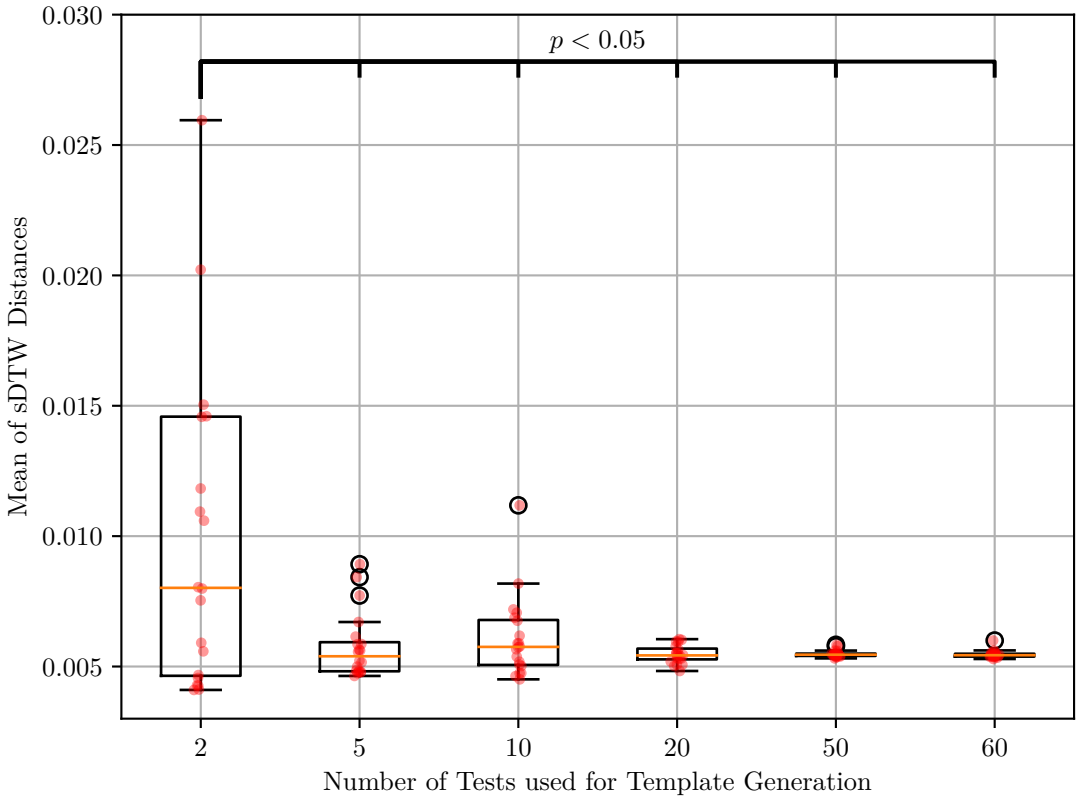

Figure 5.1: Template Group Evaluation. For each template of the Groups G_n with $n \in (2, 5, 10, 20, 50, 60)$ the mean sDTW distance to all sessions in the template evaluation test sets was calculated. Outliers above values of 0.03 were excluded. Red dots represent the mean of sDTW distances of one template t. Only template group G_2 showed significant differences of the values to all other groups.

Furthermore in Figure 5.2 three different exemplary templates are shown. Template (A) contains three smooth peaks, while template (B) also contains three peaks, where on top of all peaks small edges are recognizable. In template (C) there are 5 bigger peaks and 1 smaller peak prominent. Groups of two peaks are somehow connected and are fused partly. For all templates the peaks occur in frequent distances, while peaks of template (A) have wider base, than peaks of both other templates. Moreover the second peak is taller for template (A) and (B).

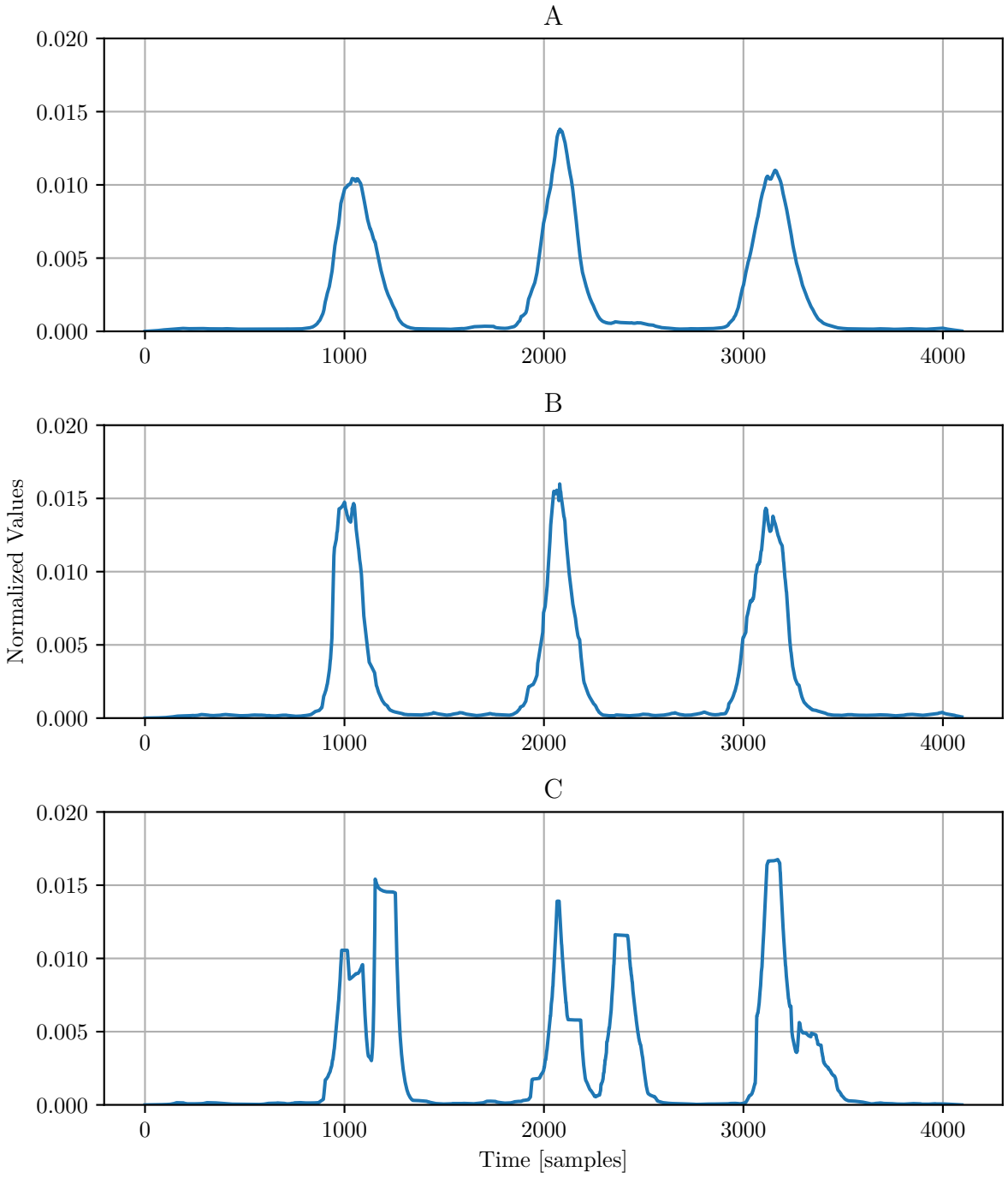

Figure 5.2: Individual Impacts on Templates. Templates from different Template Groups G_n are shown. While in template (A) of group G_{60} and template (B) of group G_5 the three peaks due to turning sequences are prominent, in template (C) of group G_2 there are six peaks.

5.1.2 Threshold Adjustment

After an optimal template t_{opt} of the group G_{opt} was generated, the test detection algorithm was performed on all 108 clinical test sessions of the test detection evaluation data set shown in Figure 4.2. In total there were 216 gait tests contained in the clinical sessions, as one session includes one 4x10m test and one two minute walking test. The detection was applied on each foot seperately so in total there were 432 tests, which should be detected. In Table 5.1 the optimal threshold and the corresponding performance measures are given for the gait test detection without postprocessing and with postprocessing.

Table 5.1: Gait Test Detection Results

	Precission	**Recall**	**F1-score**	**Threshold**
without Postprocessing	85.2 %	91.4 %	86.9 %	0.013
with Postprocessing	91.9 %	91.7 %	93.4 %	0.029

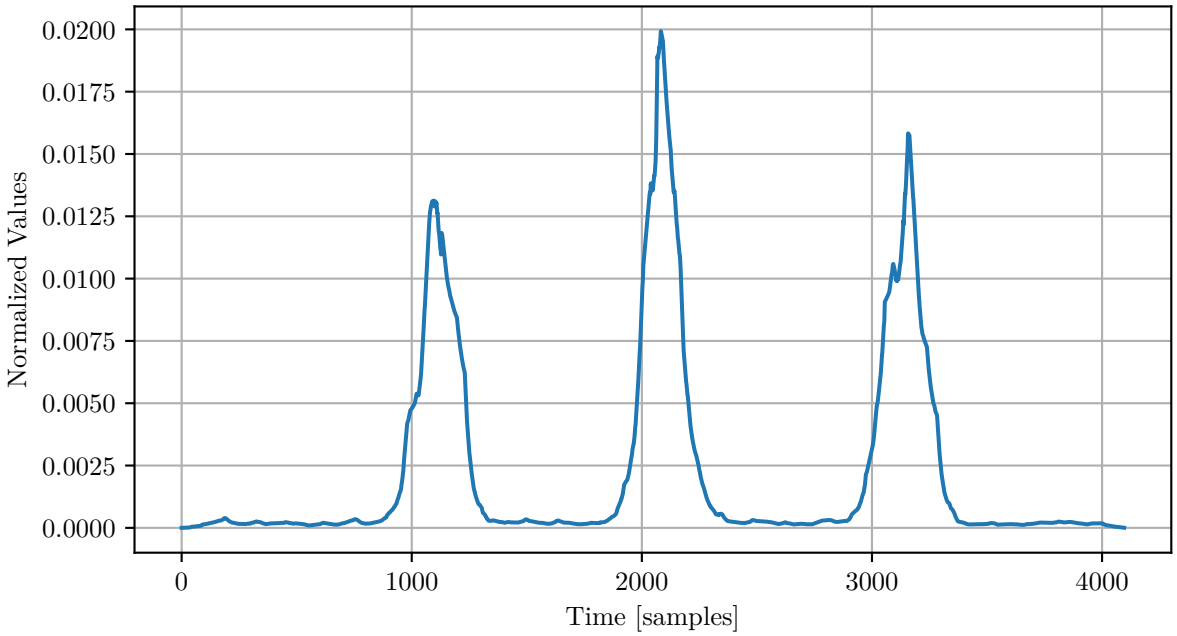

Figure 5.3: Generated optimal Template t_{opt}. One examplary template t_{opt} of group G_5. This template was used to optimize the thresholds in Table 5.1.

5.2 Macro Parameter Calculation

The WB definitions of Orendurff et al. [Ore08] and Del Din et al. [Del17] were used for generating WB sequences in the home-monitoring data which was introduced in Section 4.2. In Figure 5.4 those both definitions have been applied to the same sequence, generating different outcomes. The upper subfigure shows a result with WB definition, now referred to as $WB_{2.5,2}$, of Del Din et al. [Del17], leading to two WBs, as the resting phase between the walking activity exceeds 2.5 seconds. On the other hand, the lower subfigure was computed with WB definition, now referred to as $WB_{10,2}$ of Orendurff et al. [Ore08], resulting in only one WB, as the resting phase is shorter than ten seconds.

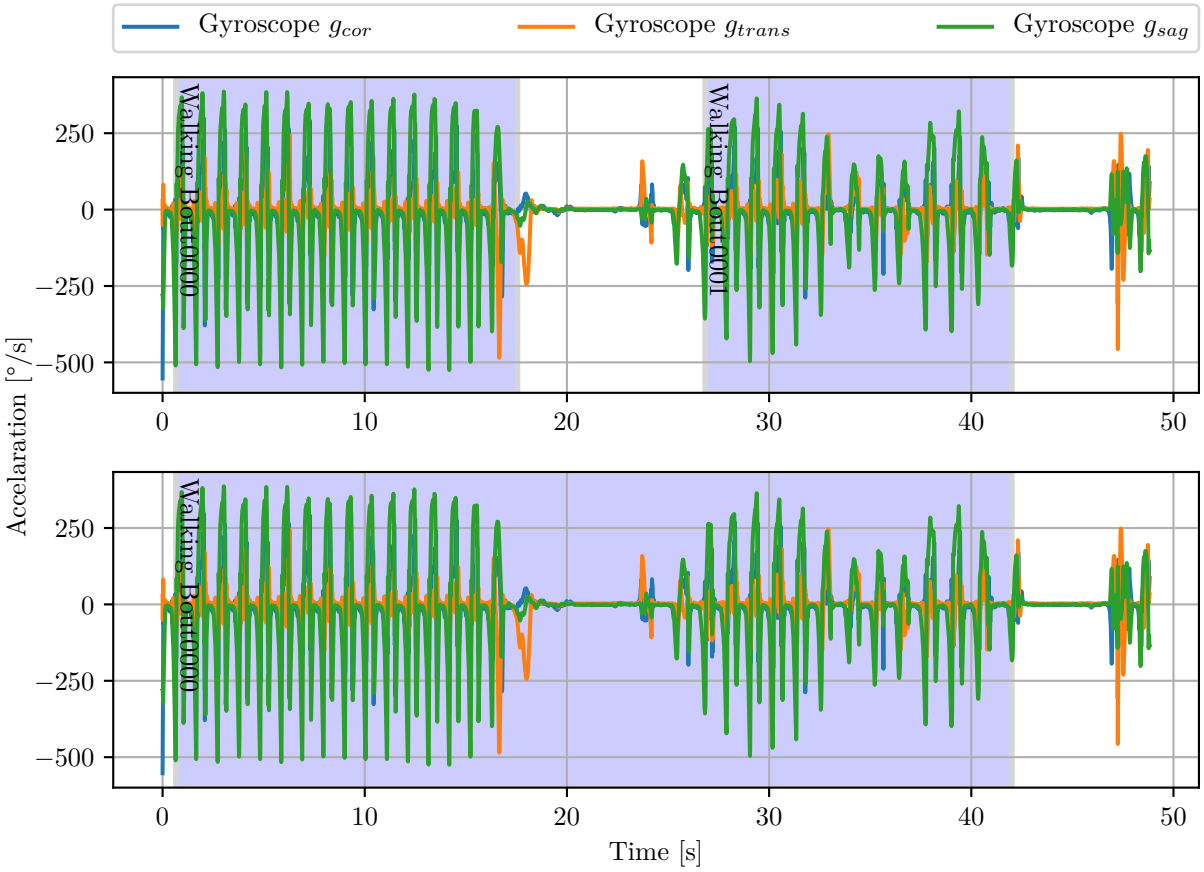

Figure 5.4: Outcomes of different WB Definitions. WBs generated on the same gait ata of the left foot. In the upper plot the WBs were compute with the WB definition $WB_{2.5,2}$, while the lower plot was computed with $WB_{10,2}$. For $WB_{2.5,2}$ two WBs were created and for $WB_{10,2}$ one WB was created.

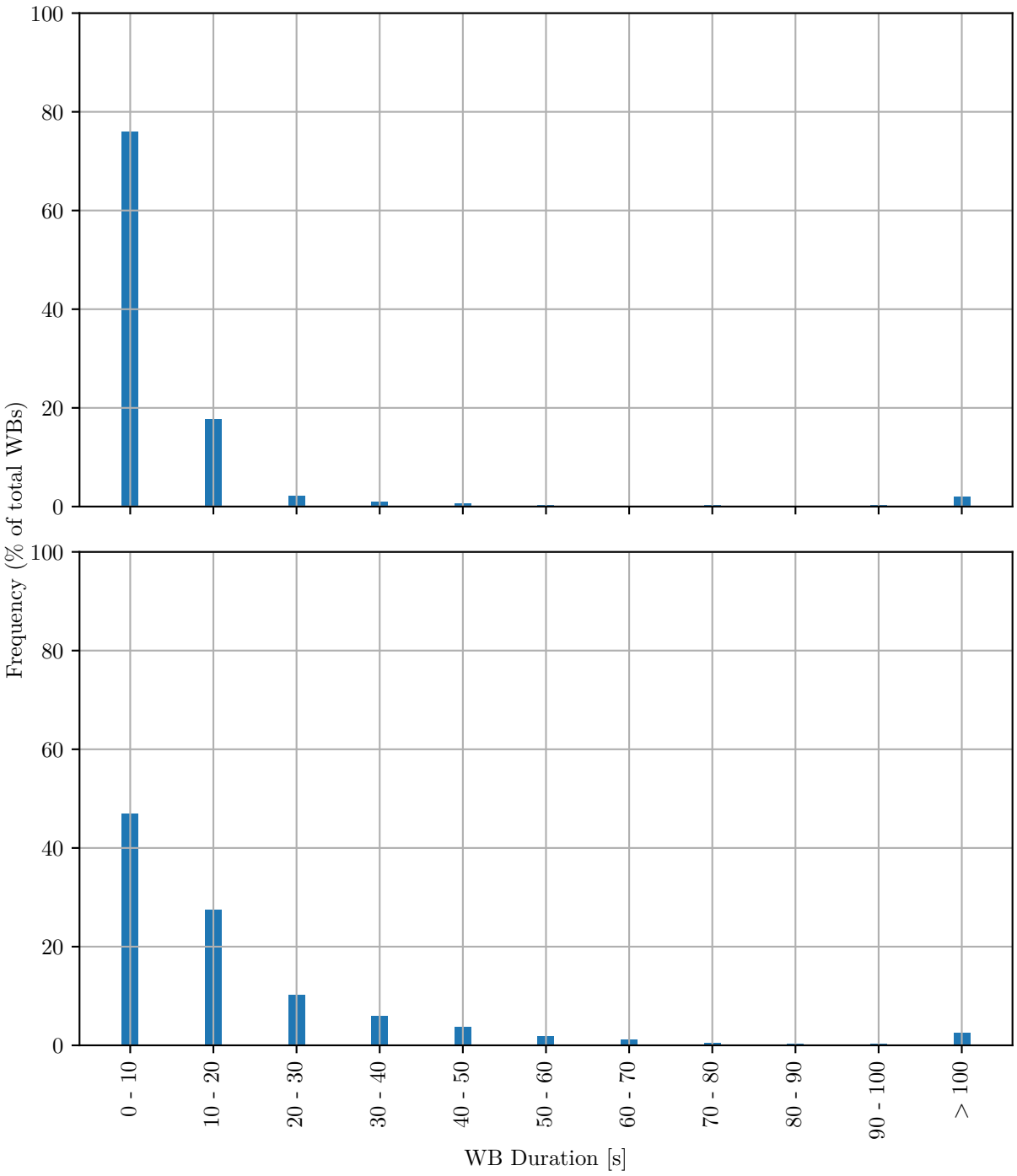

Figure 5.5: Effect of different WB Definitions on Number of WBs. Due to different MRPs of the WB definitions the number of generated WBs differ. The upper plot is calculated with WB definition $WB_{2.5,2}$ of a shorter MRP of 2.5 seconds and the lower plot with WB definition $WB_{10,2}$ with a longer MRP of 10 seconds.

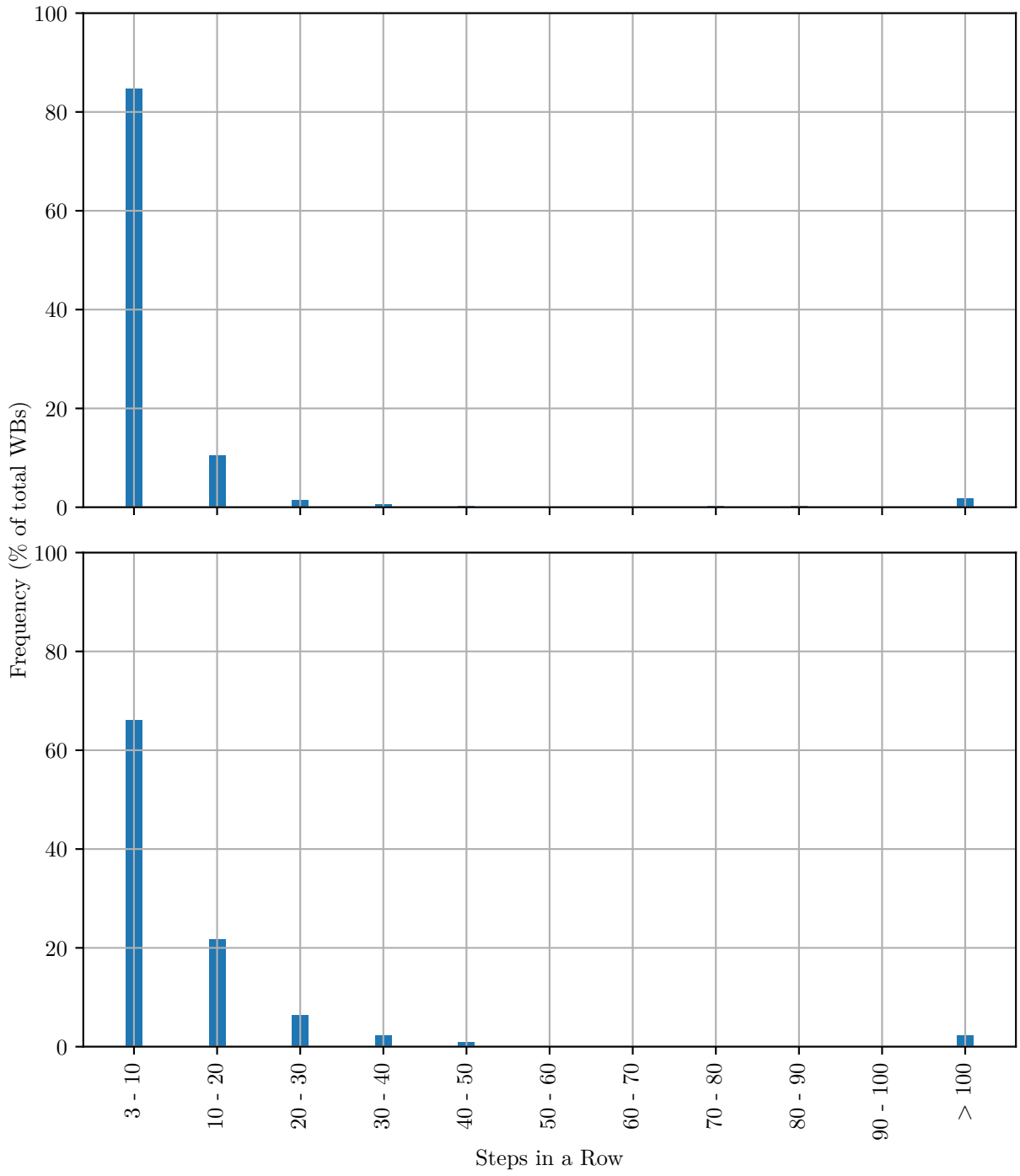

Figure 5.6: Effect of different WB Definitions on Number of Steps in a Row. Effect of different WB definitions (upper plot: $WB_{2.5,2}$, lower plot: $WB_{10,2}$) on the amount of steps in a row. A higher MRP, which is used in the lower plot, led to a more spread distribution.

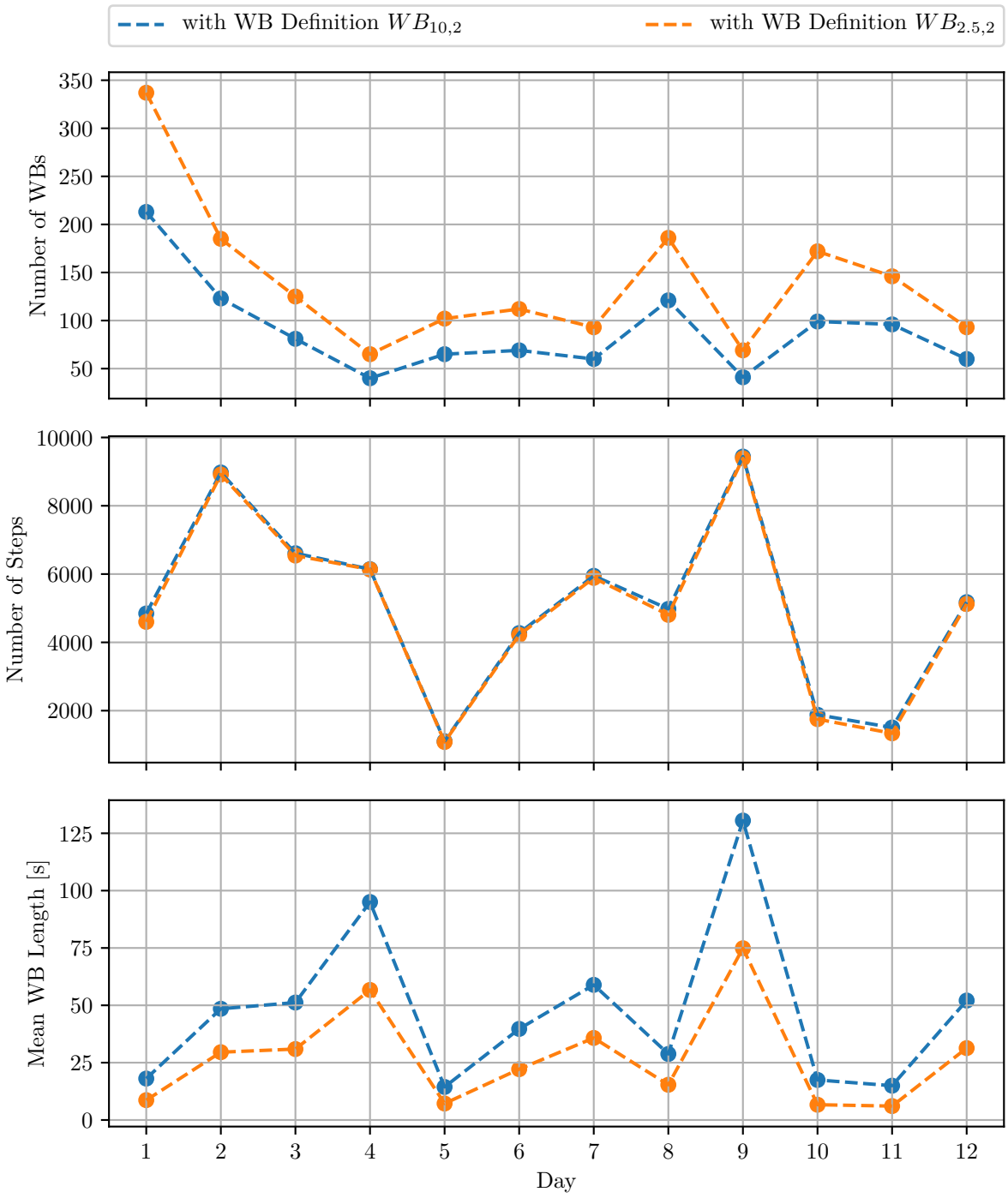

Figure 5.7: Macro Parameters on each Day. Differences that occur by using different WB definitions. The blue samples are generated by a WB definition $WB_{10,2}$ with a higher MRP value than the orange samples of $WB_{2.5,2}$.

Results of the macro parameter calculation can be seen in Figure 5.5, 5.6, Figure 5.7 and Figure 5.5.

For different WB definitions the outcomes of macro characteristics differ. Regarding the *number of WBs*, WB definitions with higher RMS result in a smaller total *number of WBs*. While definition $WB_{2.5,2}$ generated in total 1685 WBs, the definition $WB_{10,2}$ only generated 1068 WBs, which is only about 63 % of the other amount.

Frequency of different WB durations is illustrated in Figure 5.5 using two different MRP values. In the upper subplot the WB definition $WB_{2.5,2}$ of Del Din et al. is used, which has a RMS value of 2.5 seconds. Furthermore, the lower subplot was computed with the WB definition $WB_{10,2}$ of Orendurff et al. [Ore08].

Using the $WB_{2.5,2}$ definition, WBs of small durations (0-20 seconds) are highly dominant. WBs with a duration between zero and ten seconds already made up about 76 % of all WBs. Including the next interval, WBs in the range of zero to twenty seconds contain about 94 % of the total amount of WBs. Sequences of longer walking (100 seconds) share 2 % of the total amount.

Contrary, observing a WB definition of higher RMS values as it is in the lower subplot of Figure 5.5, the output differs. The sum of WBs in the iterval of zero to twenty seconds contains only 74 % of the total number. The trend is tending to a more wider distribution of WB regarding WB durations.

Observing the characteristic of *steps in a row* for these two walking bout definitions a similar trend is obtained. Due to the used WB definitions, the minimum number of steps was set to 3 steps, as explained in Section 4.2. Most prominent are three to ten *steps in a row*, which contain 85 % for $WB_{2.5,2}$ and 66 % for $WB_{10,2}$. For both definitions sequences of long walking, containing of more than 100 steps, made up about 2 % of all WBs.

Furthermore, the macro parameters *number of WBs*, *number of steps* and *mean WB length* are compared for $WB_{2.5,2}$ and $WB_{10,2}$ for each day seperately. In Figure 5.7 these parameters are plotted over each day. The blue lines are the parameters created with $WB_{10,2}$ and the orange lines of $WB_{2.5,2}$ respectively.

The number of WBs is increasing for lower MRP values. For some days the *number of WBs* almost doubles. The *number of WBs* range between 65 and 337 for $WB_{2.5,2}$ and between 40 and 213 for $WB_{10,2}$, which is a decline of 63 ± 3 % for each day.

The daily number of steps differs only in a slight way, where the *number of steps* is higher for $WB_{10,2}$. In total for $WB_{10,2}$ the amount of steps is 30441, while for $WB_{2.5,2}$ 29894 steps were detected, which are 547 steps less.

The third macro parameter is the *mean WB lenght*. Here the WB definitions of higher RMS

values obtain higher mean WB lengths. Values ranged for $WB_{10,2}$ between 14.4 and 130.5 seconds, while values for $WB_{2.5,2}$ ranged between 6.0 and 74.9 seconds, which is a decline of 54 $\pm$ 8 %.

Chapter 6

Discussion

The results for the gait test detection and the macro parameter calculation will be discussed in the next chapter.

6.1 Gait Test Detection

One goal of this thesis was the automatic detection of gait tests. The results of the detection algorithm will be discussed in the following section. The algorithm works on a signal processing basis. The gait test detection obtained good results, performing with a F1-score of 93.4 % on clinical data, applying the sDTW to a new application field.

Besides that, the DTW algorithm has already been used for stride segmentation, for example Barth et al. [Bar17]. They achieved a F1-score of 98 % for stride segmentation observing a gait test, while many other researchers used a peak detection approach for stride segmentation like Salarian et al. [Sal04], which have 5 to 15 % lower scores than the DTW method. Furthermore the DTW approach of Barth et al. shows a higher robustness also performing quiete well on free-living gait data obtaining a F1-score of 97 %.

Comparing this DTW-method to the gait test detection of this thesis, several differences occur. While the signals of one single step all share a very similar pattern, the gait test can differ in patterns in more different ways. Varying *numbers of steps* appear between the turning sequences, also the number of turning steps can change. Both patterns, stride and gait test differ in speeds for each subject. This problem is tackled with the use of DTW, as it is an algorithm to compare two signal sequences which vary in time or speed [Mye81]. Aligning the signal on the time axis by warping will create high similarity between those patterns.

For comparing the template with input sequences, a preprocessing substep was developed to

suppress patient-individual aspects, that lead to differences between different gait test signals. Therefore input sequences were segmentated with a gait interval segmentation.

The gait interval segmentation process was needed for two reasons. Firstly, DTW algorithm is a very memory-consuming algorithm which may lead to a processor error, as the processor can not acquire enough memory. Therefore, the complete gait signal is sliced in junks of gait intervals, which are processable. On the other hand, this segmentation was also used for accurate segmentation of gait tests. The window size of five seconds used for the gait interval segmentation detected gait test's start and stop setting soft gait test borders. In this step problems will occur, if the patient do not stops motion for at least five seconds. In the case of no rest a segment would span over multiple gait test and therefore only one gait test will be detected.

After the sDTW distance is calculated and is lower than the threshold θ a postprocessing step is applied on the remaining test candidates. This was done to distinguish between the different test types and also to check several constraints. Those constraints were needed as the DTW method also recognized non-test sequences which contain three turning sequences. Those false detected intervals are included in the Table 5.1 for the gait test detection without postprocessing. Adding those constraints results in an increase of the F1-score by 6.5 %.

6.1.1 Template Creation

Another aspect of this study was creating a template which can distinguish well between gait tests and free-living gait in general. The aim was to generate a template, which have accurate outcomes for unseen data and can be reproduced for different sensor systems or new types of gait tests.

Therefore, the different template groups G_j were created and evaluated by their group mean sDTW distance to the 4x10m tests of the template evaluation data set. A low mean distance is assumed to identify a good template group as lower sDTW distances represent a high similarity between input and template sequence.

In Figure 5.1 all those sDTW distances are plotted. The lowest group mean was the one of group G_{60}, but there was no significant difference between all groups except for group G_2. Our assumption is that no new information is gained by adding more preprocessed tests to the template. As this sDTW based test detection should be easily applied to new systems, also the required amount of data should be as small as possible. Therefore, template group G_5 was found to be the optimal group G_{opt}, as it had lowest number of test sets used for generation and the lowest group mean, that signifantly differs from previous template groups (G_2).

Furthermore, the decreasing standard deviations for higher number of tests can partly be explained by the size of the template creation set from Figure 4.2, which contained 70 test sets.

As more often the same test sets are used to create templates, also the mean sDTW distance will scatter less and less.

Moreover, the template with the lowest mean of sDTW distances is in group G_2. For optimization on specific systems, the author suggests to use the best template $t_{j,m}$, which has the global minimum of sDTW distances. This template may achieve the best perfomance.

In Figure 5.2 there are different examplary results of templates illustrated. Template (A) has the smoothest pattern, as it contains the highest number of test sets for creation. As more sets are used for averaging the template, the template illustrates a more general shape of all templates. There is also an effect of smoothing recognizable, that lead to smaller amplitude and wider bases of the peaks. Template (B) was made up of 5 different test sets. Small edges at the top of the peak refer to small distances along the time axis of the different test sets' peaks to respcetive other peaks. This effect is even more prominent for template (C), which was generated of two test sets. Three pairs of peeks occur, leading to higher sDTW distances. Those peaks may be explained by different walking speeds during test performance and also varying angular velocity of turning steps in the turning sequence.

6.1.2 DTW Algorithm Limitations

A problem that occurs, is based on the time independency of the sDTW algorithm. If the segmentated gait interval is containing three turning sequences like they appear in the 4x10m test or the two minute walking sequence, those segments are also likely to be detected as a gait test, no matter if the turning sequences appear in a periodic distance. Here the introcution of a local weight vector to the recursive cost calculation may achieve more accurate outcomes [Mül16]. By raising the costs for vertical and horizontal steps, the diagonal direction gets favorized, making stretching and squeezing of the temporal axis more expensive.

Furthermore, it is not granted that the cheapest warping path, produced by the sDTW algorithm, includes three peaks. In some cases, the turning sequences of the input sequence can be cut off, due to assignment of a single template sample to many consecutive samples of the input sequence and vice versa [Mül10]. This is the case if the warping path is stuck in one of the sequences while moving on in the other sequence. The peak due to the turning sequence is then eleminated by warping and the output sDTW distance is not meaningful in those cases. An optimal warping path would be a diagonal line without any vertical or horizontal steps, which would mean that template and input sequence are identical. To tackle this problem a different step size could be used, that forbids steps in horizontal or vertical direction. A step size which is able to do so is illustrated in Figure 6.1.

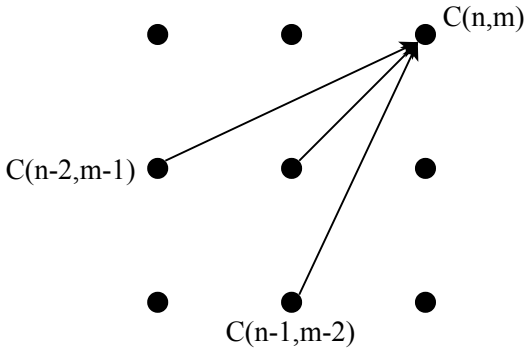

Figure 6.1: Alternative Step Size Condition. This step size condition suppresses time degenerations.

6.2 Macro Parameter Calculation

Outcomes of measuring the free-living gait data support the work of previous research done in the field of macro gait analysis. Due to the fact that only data of one PD patient was available, the results are compared to already existing research findings.

The results of the parameters *steps in a row* and *number of WBs* over one week can be compared to the results of Orendurff et al. [Ore08], as the WB definition $WB_{10,2}$ is used in both works. For both parameters the results of both studies differ slightly, as our PD patient tended to a higher number of shorter WBs ($<$ 20 seconds), which also affected the parameter *steps in a row* [Ore08]. Lower numbers of linked steps had higher frequency in our study. *Number of WBs* of healthy subjects of Orendurff et al. between 0 - 30 sechonds was 60 % of the total WB amount. Our patient's share of those Wbs from the total was already 84 % [Ore08]. This is in agreement with the work of Lord et al. [Lor13a] that PD patients tend to walk short WBs ($<$ 30 seconds), which also affects the number of *steps in a row*.

Besides that, also Del Din et al. observed the frequency of WBs of different durations with the WB definition $WB_{2.5,2}$. The total share of WBs shorter than 10 seconds was 59 % for their PD patients, while the respective share of our study was 76 %. This difference may result from the fact, that our patient did not wear the sensor the whole day, possibly excluding walking activity. Another aspect is that our study only contains one single PD patient, which may tend to shorter WBs.

Comparing outcomes of macro parameters for the two WB definitions $WB_{2.5,2}$ and $WB_{10,2}$ with MRP of 2.5 and 10 seconds, the findings support the outcomes of Barry et al. that different MRP values lead to strong differences in outcome parameters [Bar15].

Two different MRPs were used to calculate the three parameter seen in Figure 5.7. The *number of WBs* were increasing for WB definitions of shorter MRP like it is illustrated in the upper subplot of Figure 5.7. Two effects can lead to different outcomes. On the one hand, small gait sequences which are near get fused to a longer WB for higher MRP values. This effect decreases the amount of WBs. And on the other hand, single steps with a small distance get fused to one WB, even if they are not linked to each other. This effect leads to a small increase of WBs. As the *number of WBs* decrease for higher MRP values, the first effect is outweighing the second one.

The *number of steps* was almost the same for both WB definition, while $WB_{2.5,2}$ had slighty lower values. This was due to the effect that more intervals containing single strides with small time gaps were fused to one WB.

Furthermore, the *number of steps* per day illustrates the subjects activity level performed on that day. The outcomes of those data is also depending strongly on the duration and type of activity the subject wore the sensors. Observing *number of WB* values, the first impression would be that the subject was very inactive on day 9, as this was one of the lowest values for *number of WBs* of all days. In contrast, this was the day the subject was most active as the *number of steps* was the highest. This is due to very long WBs, here multiple occuring of linked gait lasting about 30 minutes, which have a huge amount of steps. On the other hand those long WBs led to smaller numbers of short WBs, as long WBs took a big share of the recorded time. The *number of steps* per day is therefore a good indetifier of how active the subject is and which type of activities the subject performs.

For the *mean WB length*, WB definition $WB_{10,2}$ produced higher values, for the same reasons mentioned before. Furthermore, this parameter also gives informations about the performed type of gait. Higher *mean WB lengths* indicates occurence of long gait sequences, like outdoor walking. Small values could represent home-environmental gait.

As macro parameters are generated by WBs also the macro outcomes change with different WB definitions, thus comparing results is quite difficult [Bar15]. For different MRP values the computed macro parameters differ in values, but both indicate the same relations and show the same trends recognizable in Figure 5.7.

Moreover, the subject wore the sensors for varying durations (time = 5.5 $\pm$ 1.7 hours) which also affects outcomes, as the study cohort of Del Din et al. and Orendurff et al. wore the sensors constantly over 7 or respectively 10 days. Thus, for our PD patient's data there may not be all daily life activities included, which affect outputs.

The existance of several different WB definitions create comparison problems and hender the progress of research in the field of macro gait analysis. To erase the comparison problem a general

WB definition should be established. This definition should satisfy the goal of gait analysis which is supporting the clinician with meaningful quantitative parameters [Lor13b]. Therefore, a WB definition should lead to outcome parameters which distinct well between impaired and non-impaired subjects. Some relations between outcome parameters and disease type, disease stage, fall history and fall prediction have been found already [Sch14, Del16, Del17, Bar17].

Chapter 7

Conclusion and Outlook

One purpose of this thesis was to develop tools to process home-monitoring data automatically. Furthermore the effect of two different WB definitions on the outcomes of macro parameters was observed.

The task to process home-monitoring data is seperating free-living gait from performed gait tests. To tackle this aspect an automatic gait test detection algorithm had to be developed. The algorithm was based on sDTW, where preprocessed segments of gait were compared to a specific generated template. If the calculated sDTW distance was lower than a predefined threshold and the input segments also fullfills several constraints, the segment was detected as a gait test.

Two different gait test had to be detected, which are the 4x10m test and the two minute walking test. Due to the fact that DTW algorithms is time-invariant, those two test types were detected simultaneously, hence both tests contain the same sequences only differing in length.

As there was a lack of home-monitoring data, this algorithm was developed and evaluated with data recorded during clinical sessions. The test detection obtained good outcomes on the clinical data, therefore applying the algorithm on home-monitoring data should be possible, even though home-monitoring's free-living gait data is unpredictable and much more complex as clinical gait data. Furthermore the performance of the gait test is highly depending on the subject's home-environment, as room barriers affect the feasibility of gait tests.

For applying that algorithm to a new sensor system a proper template from gait test data recorded with those sensors has to be generated, as computed in Section 4.1.2. Furthermore the threshold has to be optimized for this new template.

For the best of my knowledge, this is the first algorithm detecting gait test in motion data. With a F1-score of 93.4 % the outcomes are valuable to facilitate the use of the home-monitoring system, as the patients do not have to set time stamps to label the gait tests. Thus, outcomes of gait

tests in home-environments in form of micro parameters will improve as they are more accurate.

On the other hand free-living gait data, which is the total home-monitoring data that remains after excluding the gait tests, is used to calculate macro parameters, that illustrates broader trends of gait signals. Those parameters quantify free-living gait characteristics. Furthermore free-living gait is said to heightened differences of PD patients and healthy subjects, in comparison to clinical gait [Del17].

For this reason different WB definitions and their effects on macro parameters were observed, as WBs are the basis on which macro parameters are calculated. Longer MRP values led to lower number of total WBs and increased the overall mean bout length. Considering the fact that in the work of Del Din et al. only WBs of durations lasting longer than 20 seconds, showed significant differences in macro parameters. A proper general WB definition should result in outcome macro parameters which distinguish between healthy and impaired subjects.

Future applications of the gait test detection are automatisation of home-monitoring systems. This could include automatic test detection and calculation of macro parameters, signalizing critical trends of the patient's disease stage, in form of macro and micro parameters. Furthermore the prediction of fall risk could be improved by an increase of data, especially free-living gait data. Besides that, preprocessing and sDTW subsections of the test detection may be applied to applications handling detection of turning sequences. Currently, only 4x10m tests and two minute walking tests are recognized, as those are the tests our home-monitoring and clinical test battery are containing of.

Appendix A

Patent

Algorithms for gait measurement with 3-axes accelerometer/-gyro in mobile devices

Publication Number	US 2017/0042453 A1
Date of Publication	February 16, 2017
Inventors	Jeffrey Tai Kin Cheung
Assignee	Hong Kong Baptist University (HK)
Abstract	The present invention relates to a method of gait measure ment using tri-axial accelerometer/gyro in mobile devices. In particular, the present invention relates to algorithms for gait measurement using tri-axial accelerometer/gyro in mobile devices for monitoring and improving the physical movement of a moving Subject.

Appendix B

Additional Figures

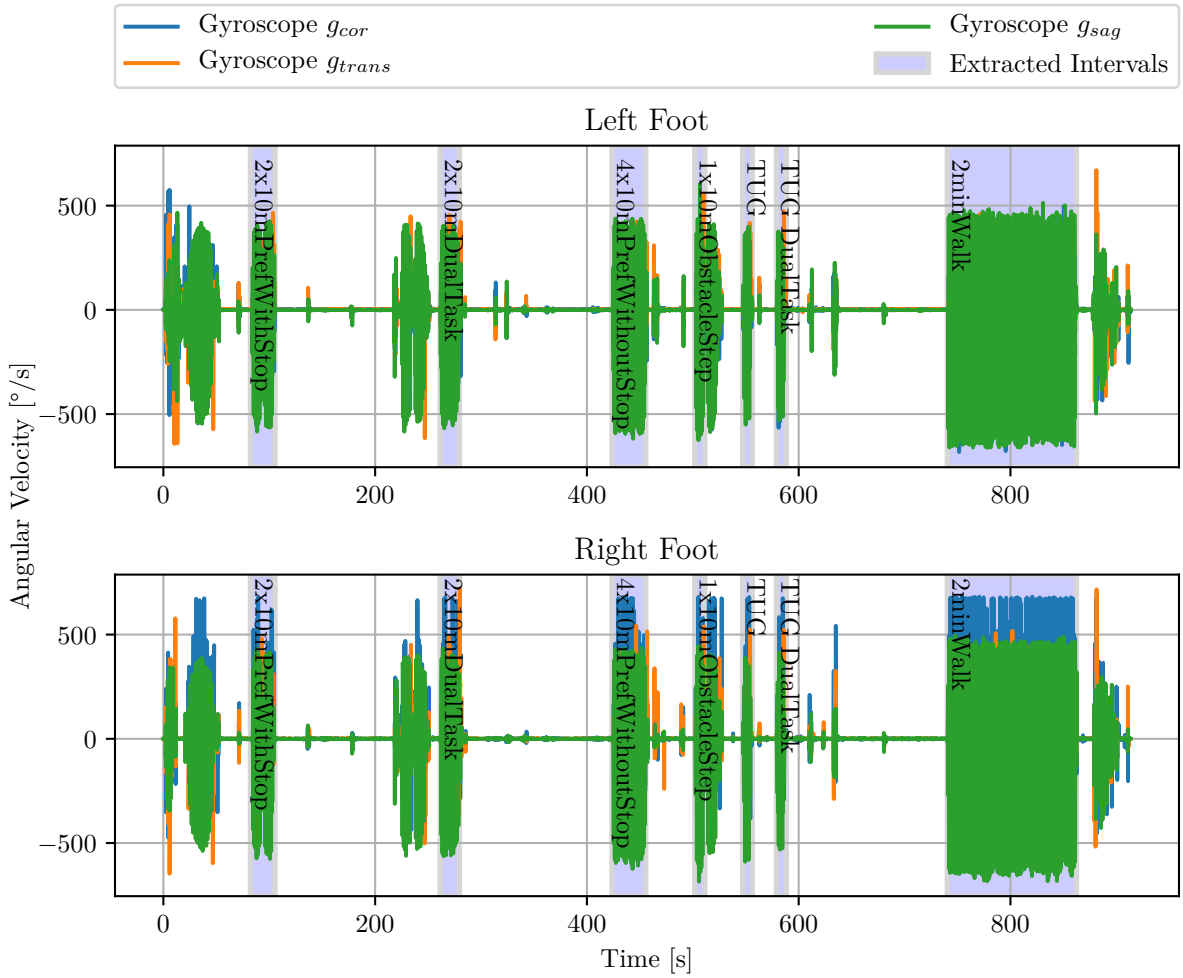

Figure B.1: Recorded clinical gait session. This clinical gait session contains seven different gait tests, which were manually labeled by the physician. One recatangular is one test with name, start and stop. Used sensors are Shimmer 2R, introdueced in Section 4.1.1.

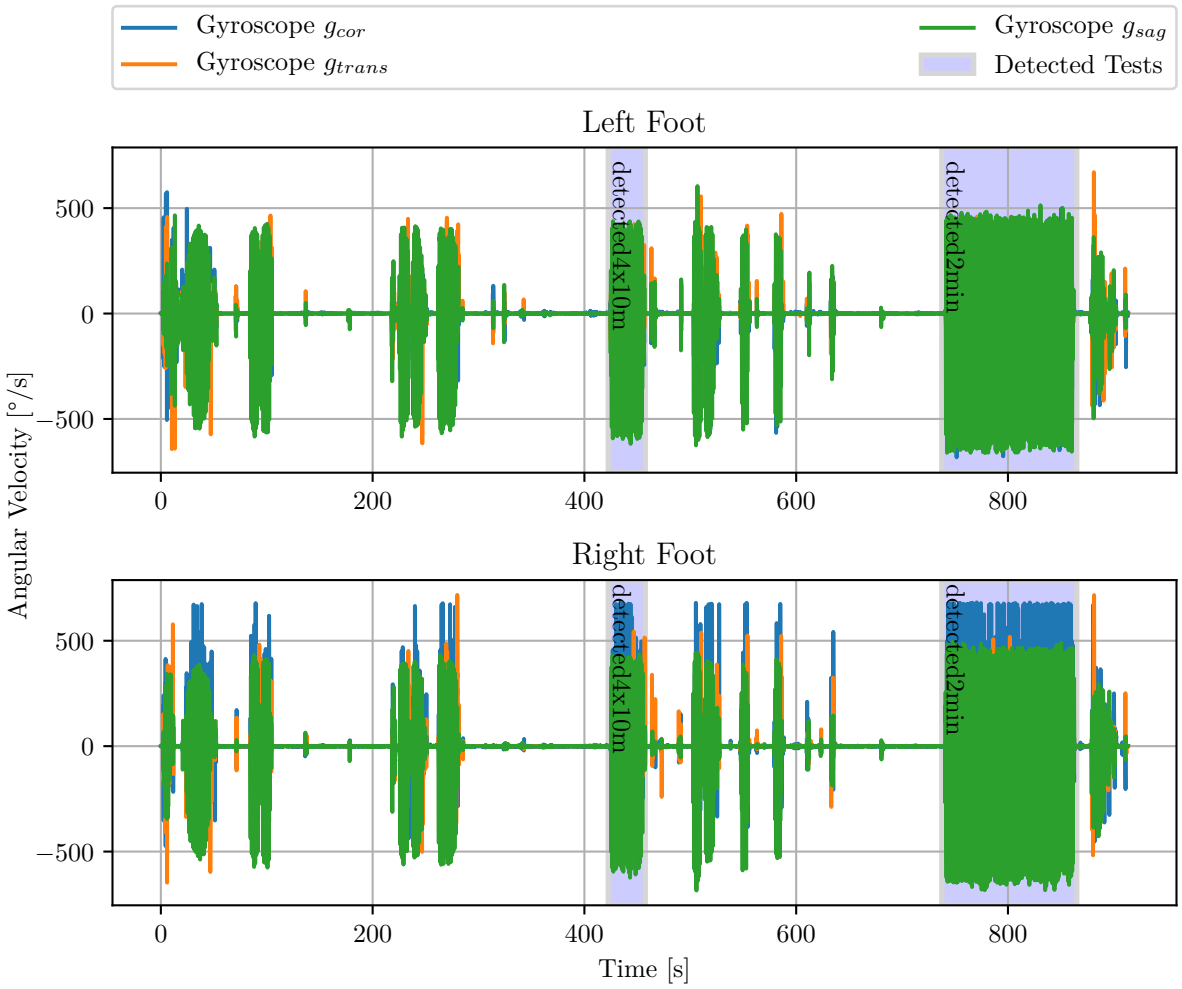

Figure B.2: Detection of Gait Tests. On the data of Figure B.1 the gait test detection algorithm was applied. The occuring 4x10m test and two minute test were detected correctly. For detection the optimized threshold $\theta = 0.025$ from Section 5.1.2 was used and as template t_{opt} on which the threshold was optimized.

Glossary

DTW Dynamic Time Warping

FOG Freezing of Gait

H&Y Hoehn and Yahr

HO Heel-Off Event

HS Heel-Strike Event

IMU Inertial Measurement Units

MRP Maximum Resting Period

MS Mid-Stance Event

PD Parkinson's Disease

sDTW subsequent Dynamic Time Warping

TO Toe-Off Event

TUG Timed Up and Go Test

UPDRS Unified Parkinson's Disease Rating Scale.

WB Walking Bout

List of Figures

List of Tables

Bibliography

[Ash01] A. Ashburn, E. Stack, R. M. Pickering, C. D. Ward: *Predicting Fallers in a Community-Based Sample of People with Parkinson's Disease*, *Gerontology*, Vol. 47, Nr. 5, 2001, pp. 277–281.

[Ata81] E. Ataman, V. Aatre, K. Wong: *Some statistical properties of median filters*, *IEEE Transactions on Acoustics, Speech, and Signal Processing*, Vol. 29, Nr. 5, oct 1981, pp. 1073–1075.

[Bac10] M. Bachlin, M. Plotnik, D. Roggen, I. Maidan, J. Hausdorff, N. Giladi, G. Troster: *Wearable Assistant for Parkinson's Disease Patients With the Freezing of Gait Symptom*, *IEEE Transactions on Information Technology in Biomedicine*, Vol. 14, Nr. 2, mar 2010, pp. 436–446.

[Bao05] M. Bao: *Analysis and design principles of MEMS devices*, Elsevier Science, 1. Issue, 2005.

[Bar15] G. Barry, B. Galna, S. Lord, L. Rochester, A. Godfrey: *Defining ambulatory bouts in free-living activity: Impact of brief stationary periods on bout metrics*, *Gait and Posture*, Vol. 42, Nr. 4, 2015, pp. 594–597.

[Bar17] J. Barth: *Automated Inertial Sensor Based Recognition and Rating of Human Gait with Emphasis on Parkinson's Disease*, Phd thesis, Friedrich-Alexander University Erlangen-Nuremberg, 2017.

[Bea09] O. Beauchet, C. Annweiler, V. Dubost, G. Allali, R. W. Kressig, S. Bridenbaugh, G. Berrut, F. Assal, F. R. Herrmann: *Stops walking when talking: a predictor of falls in older adults?*, *European Journal of Neurology*, Vol. 16, Nr. 7, jul 2009, pp. 786–795.

[Bec97] D. Beckers, J. Deckers: *Ganganalyse und Gangschulung : therapeutische Strategien für die Praxis*, Springer, 1997.

[Ber01] A. Berardelli, J. C. Rothwell, P. D. Thompson, M. Hallett: *Pathophysiology of bradykinesia in Parkinson's disease.*, *Brain : a journal of neurology*, Vol. 124, Nr. Pt 11, nov 2001, pp. 2131–46.

[Bhi12] R. Bhidayasiri, D. Tarsy: *Parkinson's Disease: Hoehn and Yahr Scale*, in *Movement Disorders: A Video Atlas*, Humana Press, Totowa, NJ, 2012, pp. 4–5.

[Bjo07] K. F. Bjornson, B. Belza, D. Kartin, R. Logsdon, J. F. McLaughlin: *Ambulatory Physical Activity Performance in Youth With Cerebral Palsy and Youth Who Are Developing Typically*, *Physical Therapy*, Vol. 87, Nr. 3, mar 2007, pp. 248–257.

[Blo01] B. R. Bloem, Y. A. Grimbergen, M. Cramer, M. Willemsen, A. H. Zwinderman: *Prospective assessment of falls in Parkinson's disease.*, *Journal of neurology*, Vol. 248, Nr. 11, nov 2001, pp. 950–8.

[Blo04] B. R. Bloem, J. M. Hausdorff, J. E. Visser, N. Giladi: *Falls and freezing of gait in Parkinson's disease: A review of two interconnected, episodic phenomena*, *Movement Disorders*, Vol. 19, Nr. 8, aug 2004, pp. 871–884.

[Boo08] T. A. Boonstra, H. van der Kooij, M. Munneke, B. R. Bloem: *Gait disorders and balance disturbances in Parkinson's disease: clinical update and pathophysiology*, *Current Opinion in Neurology*, Vol. 24, Nr. 4, aug 2008, pp. 461–471.

[Bra06] H. Braak, J. R. Bohl, C. M. Müller, U. Rüb, R. A. de Vos, K. Del Tredici: *Stanley Fahn Lecture 2005: The staging procedure for the inclusion body pathology associated with sporadic Parkinson's disease reconsidered*, *Movement Disorders*, Vol. 21, Nr. 12, dec 2006, pp. 2042–2051.

[Bro07] E. Broussolle, P. Krack, S. Thobois, J. Xie-Brustolin, P. Pollak, C. G. Goetz: *Contribution of Jules Froment to the study of Parkinsonian rigidity*, *Movement Disorders*, Vol. 22, Nr. 7, apr 2007, pp. 909–914.

[Bro15] M. A. Brodie, S. R. Lord, M. J. Coppens, J. Annegarn, K. Delbaere: *Eight-Week Remote Monitoring Using a Freely Worn Device Reveals Unstable Gait Patterns in Older Fallers*, *IEEE Transactions on Biomedical Engineering*, Vol. 62, Nr. 11, nov 2015, pp. 2588–2594.

[Bro16] M. A. D. Brodie, M. J. M. Coppens, S. R. Lord, N. H. Lovell, Y. J. Gschwind, S. J. Redmond, M. B. Del Rosario, K. Wang, D. L. Sturnieks, M. Persiani, K. Delbaere:

Wearable pendant device monitoring using new wavelet-based methods shows daily life and laboratory gaits are different, *Medical & Biological Engineering & Computing*, Vol. 54, Nr. 4, apr 2016, pp. 663–674.

[Bro17] M. A. Brodie, M. J. Coppens, A. Ejupi, Y. J. Gschwind, J. Annegarn, D. Schoene, R. Wieching, S. R. Lord, K. Delbaere: *Comparison between clinical gait and daily-life gait assessments of fall risk in older people*, *Geriatrics & Gerontology International*, Vol. 17, Nr. 11, nov 2017, pp. 2274–2282.

[Cav07] J. T. Cavanaugh, K. L. Coleman, J. M. Gaines, L. Laing, M. C. Morey: *Using Step Activity Monitoring to Characterize Ambulatory Activity in Community-Dwelling Older Adults*, *Journal of the American Geriatrics Society*, Vol. 55, Nr. 1, jan 2007, pp. 120–124.

[Che16] S. Chen, J. Lach, B. Lo, G.-Z. Yang: *Toward Pervasive Gait Analysis With Wearable Sensors: A Systematic Review*, *IEEE Journal of Biomedical and Health Informatics*, Vol. 20, Nr. 6, nov 2016, pp. 1521–1537.

[Dan14] K. A. Danks, M. A. Roos, D. McCoy, D. S. Reisman: *A step activity monitoring program improves real world walking activity post stroke*, 2014.

[Del16] S. Del Din, A. Godfrey, B. Galna, S. Lord, L. Rochester: *Free-living gait characteristics in ageing and Parkinson's disease: impact of environment and ambulatory bout length.*, *Journal of neuroengineering and rehabilitation*, Vol. 13, Nr. 1, 2016, pp. 46.

[Del17] S. Del Din, B. Galna, A. Godfrey, E. M. J. Bekkers, E. Pelosin, F. Nieuwhof, A. Mirelman, J. M. Hausdorff, L. Rochester: *Analysis of Free-Living Gait in Older Adults With and Without Parkinson's Disease and With and Without a History of Falls: Identifying Generic and Disease-Specific Characteristics*, *The Journals of Gerontology: Series A*, Vol. 00, Nr. 00, 2017, pp. 1–7.

[Der10] M. Derawi, P. Bours, K. Holien: *Improved cycle detection for accelerometer based gait authentication*, in *2010 Sixth International Conference on Intelligent Information Hiding and Multimedia Signal Processing*, 2010, pp. 312–317.

[Esk17] B. Eskofier, S. Lee, M. Baron, A. Simon, C. Martindale, H. Gaßner, J. Klucken, B. M. Eskofier, S. I. Lee, M. Baron, A. Simon, C. F. Martindale, H. Gaßner, J. Klucken: *An Overview of Smart Shoes in the Internet of Health Things: Gait and Mobility Assessment in Health Promotion and Disease Monitoring*, *Applied Sciences*, Vol. 7, Nr. 10, sep 2017, pp. 986.

[Fer95] F. Ferraris, U. Grimaldi, M. Parvis: *Sensors and materials : an international journal on sensor technology.*, Vol. 7, Scientific Publ. Division of MYU, 1995.

[Gil01] N. Giladi, T. A. Treves, E. S. Simon, H. Shabtai, Y. Orlov, B. Kandinov, D. Paleacu, A. D. Korczyn: *Freezing of gait in patients with advanced Parkinson's disease*, *Journal of Neural Transmission*, Vol. 108, Nr. 1, jan 2001, pp. 53–61.

[Goe04] C. G. Goetz, W. Poewe, O. Rascol, C. Sampaio, G. T. Stebbins, C. Counsell, N. Giladi, R. G. Holloway, C. G. Moore, G. K. Wenning, M. D. Yahr, L. Seidl: *Movement Disorder Society Task Force report on the Hoehn and Yahr staging scale: Status and recommendations The Movement Disorder Society Task Force on rating scales for Parkinson's disease*, *Movement Disorders*, Vol. 19, Nr. 9, sep 2004, pp. 1020–1028.

[Goe08] C. G. Goetz, B. C. Tilley, S. R. Shaftman, G. T. Stebbins, S. Fahn, P. Martinez-Martin, W. Poewe, C. Sampaio, M. B. Stern, R. Dodel, B. Dubois, R. Holloway, J. Jankovic, J. Kulisevsky, A. E. Lang, A. Lees, S. Leurgans, P. A. LeWitt, D. Nyenhuis, C. W. Olanow, O. Rascol, A. Schrag, J. A. Teresi, J. J. van Hilten, N. LaPelle, Movement Disorder Society UPDRS Revision Task Force: *Movement Disorder Society-sponsored revision of the Unified Parkinson's Disease Rating Scale (MDS-UPDRS): Scale presentation and clinimetric testing results*, *Movement Disorders*, Vol. 23, Nr. 15, nov 2008, pp. 2129–2170.

[Hal98] S. Halliday, D. Winter, J. Frank, A. Patla, F. Prince: *The initiation of gait in young, elderly, and Parkinson's disease subjects*, *Gait & Posture*, Vol. 8, Nr. 1, 1998, pp. 8–14.

[Heg16] N. Hegde, M. Bries, E. Sazonov, N. Hegde, M. Bries, E. Sazonov: *A Comparative Review of Footwear-Based Wearable Systems*, *Electronics*, Vol. 5, Nr. 4, aug 2016, pp. 48.

[Kan14] C. Kanzler: *Validation of an Inertial Sensor based Calculation of 3D Gait Parameters with a Motion Capture System.*, Bachelor thesis, Friedrich-Alexander University Erlangen-Nuremberg, 2014.

[Kar06] D. Karantonis, M. Narayanan, M. Mathie, N. Lovell, B. Celler: *Implementation of a Real-Time Human Movement Classifier Using a Triaxial Accelerometer for Ambulatory Monitoring*, *IEEE Transactions on Information Technology in Biomedicine*, Vol. 10, Nr. 1, jan 2006, pp. 156–167.

[Ker10] G. K. Kerr, C. J. Worringham, M. H. Cole, P. F. Lacherez, J. M. Wood, P. A. Silburn: *Predictors of future falls in Parkinson disease*, *Neurology*, Vol. 75, Nr. 2, jul 2010, pp. 116–124.

[Klu13] J. Klucken, J. Barth, P. Kugler, J. Schlachetzki, T. Henze, F. Marxreiter, Z. Kohl, R. Steidl, J. Hornegger, B. Eskofier, J. Winkler: *Unbiased and Mobile Gait Analysis Detects Motor Impairment in Parkinson's Disease*, *PLoS ONE*, Vol. 8, Nr. 2, feb 2013, pp. e56956.

[Klu15] J. Klucken, K. E. Friedl, B. M. Eskofier, J. M. Hausdorff: *Guest Editorial: Enabling Technologies for Parkinson's Disease Management.*, *IEEE journal of biomedical and health informatics*, Vol. 19, Nr. 6, nov 2015, pp. 1775–6.

[Koh01] R. Kohavi: *A Study of Cross-Validation and Bootstrap for Accuracy Estimation and Model Selection*, Vol. 14, Morgan Kaufmann, mar 2001.

[Lim05] L. Lim, E. V. Wegen, C. De Goede: *Measuring gait and gait-related activities in Parkinson's patients own home environment: a reliability, responsiveness and feasibility study*, *Parkinsonism & related disorders*, Vol. 11, Nr. 1, 2005, pp. 19–24.

[Lor13a] S. Lord, B. Galna, J. Verghese, S. Coleman, D. Burn, L. Rochester: *Independent Domains of Gait in Older Adults and Associated Motor and Nonmotor Attributes: Validation of a Factor Analysis Approach*, *The Journals of Gerontology Series A: Biological Sciences and Medical Sciences*, Vol. 68, Nr. 7, jul 2013, pp. 820–827.

[Lor13b] S. Lord, B. Galna, L. Rochester: *Moving forward on gait measurement: Toward a more refined approach*, *Movement Disorders*, Vol. 28, Nr. 11, sep 2013, pp. 1534–1543.

[Lor16] S. Lord, B. Galna, A. J. Yarnall, S. Coleman, D. Burn, L. Rochester: *Predicting first fall in newly diagnosed Parkinson's disease: Insights from a fall-naïve cohort*, *Movement Disorders*, Vol. 31, Nr. 12, dec 2016, pp. 1829–1836.

[McD05] C. M. McDonald, L. Widman, R. T. Abresch, S. A. Walsh, D. D. Walsh: *Utility of a step activity monitor for the measurement of daily ambulatory activity in children*, *Archives of Physical Medicine and Rehabilitation*, Vol. 86, Nr. 4, apr 2005, pp. 793–801.

[Mül10] M. Müller: *Information retrieval for music and motion*, Springer, 2010.

[Mül16] M. Müller: *Fundamentals of Music Processing : audio, analysis, algorithms, applications.*, Springer, 2016.

[Mus08] D. Muslimović, B. Post, J. D. Speelman, B. Schmand, R. J. de Haan: *Determinants of disability and quality of life in mild to moderate Parkinson disease*, *Neurology*, Vol. 70, Nr. 23, jun 2008, pp. 2241 LP – 2247.

[Mye81] C. Myers, L. Rabiner: *A comparative study of several dynamic time-warping algorithms for connected-word recognition*, *The Bell System Technical Journal*, Vol. 60, Nr. 7, 1981, pp. 1389–1409.

[Naj03] B. Najafi, K. Aminian, A. Paraschiv-Ionescu, F. Loew, C. J. Büla, P. Robert: *Ambulatory system for human motion analysis using a kinematic sensor: Monitoring of daily physical activity in the elderly*, *IEEE Transactions on Biomedical Engineering*, Vol. 50, Nr. 6, 2003, pp. 711–723.

[Ore08] M. S. Orendurff: *How humans walk: Bout duration, steps per bout, and rest duration*, *The Journal of Rehabilitation Research and Development*, Vol. 45, Nr. 7, 2008, pp. 1077–1090.

[Pan85] J. Pan, W. Tompkins: *A real-time QRS detection algorithm*, *EEE Transactions on Biomedical Engineering*, Vol. 32, Nr. 3, 1985, pp. 230–236.

[Pos07] B. Post, M. P. Merkus, R. J. de Haan, J. D. Speelman, CARPA Study Group: *Prognostic factors for the progression of Parkinson's disease: A systematic review*, *Movement Disorders*, Vol. 22, Nr. 13, oct 2007, pp. 1839–1851.

[Ram02] C. Ramaker, J. Marinus, A. M. Stiggelbout, B. J. van Hilten: *Systematic evaluation of rating scales for impairment and disability in Parkinson's disease*, *Movement Disorders*, Vol. 17, Nr. 5, sep 2002, pp. 867–876.

[Ram14] A. Rampp, J. Barth, S. Schülein, K. Gassmann, J. Klucken, B. Eskofier: *Inertial Sensor-Based Stride Parameter Calculation From Gait Sequences in Geriatric Patients*, *IEEE transactions on bio-medical engineering*, nov 2014.

[Roo12] M. A. Roos, K. S. Rudolph, D. S. Reisman: *The Structure of Walking Activity in People After Stroke Compared With Older Adults Without Disability: A Cross-Sectional Study*, *Physical Therapy*, Vol. 92, Nr. 9, sep 2012, pp. 1141–1147.

[Ros97] R. Rosin, H. Topka, J. Dichgans: *Gait initiation in parkinson's disease*, *Movement Disorders*, Vol. 12, Nr. 5, sep 1997, pp. 682–690.

[Rov17] E. Rovini, C. Maremmani, F. Cavallo: *How Wearable Sensors Can Support Parkinson's Disease Diagnosis and Treatment: A Systematic Review*, *Frontiers in Neuroscience*, Vol. 11, oct 2017, pp. 555.

[Sab05] A. Sabatini, C. Martelloni, S. Scapellato, F. Cavallo: *Assessment of Walking Features From Foot Inertial Sensing*, *IEEE Transactions on Biomedical Engineering*, Vol. 52, Nr. 3, mar 2005, pp. 486–494.

[Sal04] A. Salarian, H. Russmann, F. Vingerhoets, C. Dehollain, Y. Blanc, P. Burkhard, K. Aminian: *Gait Assessment in Parkinson's Disease: Toward an Ambulatory System for Long-Term Monitoring*, *IEEE Transactions on Biomedical Engineering*, Vol. 51, Nr. 8, aug 2004, pp. 1434–1443.

[Sch00] A. Schrag, M. Jahanshahi: *What contributes to quality of life in patients with Parkinson's disease?*, *Journal of Neurology, Neurosurgery & Psychiatry*, Vol. 69, Nr. 1, 2000, pp. 308–312.

[Sch06] A. Schrag: *Quality of life and depression in Parkinson's disease*, *Journal of Neurological Sciences*, Vol. 248, Nr. 1, 2006, pp. 151–157.

[Sch14] M. Schwenk, K. Hauer, T. Zieschang, S. Englert, J. Mohler, B. Najafi: *Sensor-derived physical activity parameters can predict future falls in people with dementia*, *Gerontology*, Vol. 60, Nr. 6, 2014, pp. 483–492.

[Shu96] L. M. Shulman, C. Singer, J. A. Bean, W. J. Weiner: *Internal tremor in patients with Parkinson's disease*, *Movement Disorders*, Vol. 11, Nr. 1, jan 1996, pp. 3–7.

[Sil16] D. F. Silva, G. E. A. P. A. Batista: *Speeding Up All-Pairwise Dynamic Time Warping Matrix Calculation*, in *Proceedings of the 2016 SIAM International Conference on Data Mining*, Society for Industrial and Applied Mathematics, Philadelphia, PA, jun 2016, pp. 837–845.

[Sko10] I. Skog, P. Händel, J. O. Nilsson, J. Rantakokko: *Zero-Velocity Detection—An Algorithm Evaluation*, *Biomedical Engineering, IEEE Transactions on*, Vol. 57, dec 2010, pp. 2657–2666.

[Sni07] A. H. Snijders, B. P. van de Warrenburg, N. Giladi, B. R. Bloem: *Neurological gait disorders in elderly people: clinical approach and classification*, *The Lancet Neurology*, Vol. 6, Nr. 1, jan 2007, pp. 63–74.

[Ste08] T. Steffen, M. Seney: *Test-Retest Reliability and Minimal Detectable Change on Balance and Ambulation Tests, the 36-Item Short-Form Health Survey, and the Unified Parkinson Disease Rating Scale in People With Parkinsonism*, *Physical Therapy*, Vol. 88, Nr. 6, jun 2008, pp. 733–746.

[Stu11] S. Studenski, S. Perera, K. Patel, C. Rosano, K. Faulkner, M. Inzitari, J. Brach, J. Chandler, P. Cawthon, E. B. Connor, M. Nevitt, M. Visser, S. Kritchevsky, S. Badinelli, T. Harris, A. B. Newman, J. Cauley, L. Ferrucci, J. Guralnik: *Gait Speed and Survival in Older Adults*, *JAMA*, Vol. 305, Nr. 1, jan 2011, pp. 50.

[Tao12] W. Tao, T. Liu, R. Zheng, H. Feng, W. Tao, T. Liu, R. Zheng, H. Feng: *Gait Analysis Using Wearable Sensors*, *Sensors*, Vol. 12, Nr. 2, feb 2012, pp. 2255–2283.

[The05] L. L. D. Thede: *Practical analog and digital filter design*, Artech House, 2005.

[TL12] C. Tudor-Locke, M. M. Brashear, P. T. Katzmarzyk, W. D. Johnson: *Peak Stepping Cadence in Free-Living Adults: 2005–2006 NHANES*, *Journal of Physical Activity and Health*, Vol. 9, Nr. 8, 2012, pp. 1125–1129.

[Ver07] J. Verghese, C. Wang, R. B. Lipton, R. Holtzer, X. Xue: *Quantitative gait dysfunction and risk of cognitive decline and dementia*, *Journal of Neurology, Neurosurgery & Psychiatry*, Vol. 78, Nr. 9, sep 2007, pp. 929–935.

[Wei09] Weidong Le, Shen Chen, J. Jankovic: *Etiopathogenesis of Parkinson Disease: A New Beginning?*, *The Neuroscientist*, Vol. 15, Nr. 1, feb 2009, pp. 28–35.

[Wei13] A. Weiss, M. Brozgol, M. Dorfman, T. Herman, S. Shema, N. Giladi, J. M. Hausdorff: *Does the Evaluation of Gait Quality During Daily Life Provide Insight Into Fall Risk? A Novel Approach Using 3-Day Accelerometer Recordings*, *Neurorehabilitation and Neural Repair*, Vol. 27, Nr. 8, oct 2013, pp. 742–752.

[Whi91] M. Whittle: *Gait analysis : an introduction*, Butterworth-Heinemann, 1991.

[Wil06] D. R. Williams, H. C. Watt, A. J. Lees: *Predictors of falls and fractures in bradykinetic rigid syndromes: a retrospective study*, *Journal of Neurology, Neurosurgery & Psychiatry*, Vol. 77, Nr. 4, apr 2006, pp. 468–473.

[Woo02] B. H. Wood, J. A. Bilclough, A. Bowron, R. W. Walker: *Incidence and prediction of falls in Parkinson's disease: a prospective multidisciplinary study.*, *Journal of neurology, neurosurgery, and psychiatry*, Vol. 72, Nr. 6, jun 2002, pp. 721–5.

[Wor13] P. F. Worth: *How to treat Parkinson's disease in 2013.*, *Clinical medicine (London, England)*, Vol. 13, Nr. 1, feb 2013, pp. 93–6.

[Zam11] C. Zampieri, A. Salarian, P. Carlson-Kuhta, J. G. Nutt, F. B. Horak: *Assessing mobility at home in people with early Parkinson's disease using an instrumented Timed Up and Go test.*, *Parkinsonism & related disorders*, Vol. 17, Nr. 4, may 2011, pp. 277–80.

[Zar02] S. Zareparsi, R. Camicioli, G. Sexton, T. Bird, P. Swanson, J. Kaye, J. Nutt, H. Payami: *Age at onset of Parkinson disease and apolipoprotein E genotypes*, *American Journal of Medical Genetics*, Vol. 107, Nr. 2, jan 2002, pp. 156–161.